Int J Clin Exp Pathol 2013;6(12):2651-2667
www.ijcep.com /ISSN:1936-2625/IJCEP1309068

Original Article

Effects and interactions of MiR-577 and TSGA10 in regulating esophageal squamous cell carcinoma

Xiang Yuan[1], Jiangtu He[4], Fenyong Sun[3], Jiang Gu[1,2]

[1]Department of Pathology, School of Basic Medical Science, Peking University, Beijing 100083, China; [2]Molecular Pathology Laboratory and Guangdong Provincial Key Laboratory of Infectious Diseases and Molecular Immunopathology, Shantou University Medical College, Shantou 515041, China; [3]Department of Clinical Laboratory Medicine, Shanghai Tenth People's Hospital of Tongji University, Shanghai 200072, China; [4]Department of Central Laboratory, Shanghai Tenth People's Hospital of Tongji University, Shanghai 200072, China

Received September 26, 2013; Accepted October 29, 2013; Epub November 15, 2013; Published December 1, 2013

Abstract: Testis specific 10 (TSGA10) was originally identified as a testis-specific protein and tumor-associated antigen in a number of cancer types. In this study, we found that down-regulation of TSGA10 was associated with increased malignancy and clinical features of esophageal squamous cell carcinomas (ESCCs). Moreover, increased expression of TSGA10 inhibited, while its knockdown promoted, tumor formation in vivo in nude mice. At the 3'UTR of the TSGA10 gene we identified two binding sites for microRNA-577 (miR-577). Further investigation demonstrated that expression levels of miR-577 and TSGA10 were negatively correlated to each other in ESCC cell lines and tumor samples. Moreover, manipulation of miR-577 and TSGA10 expression confirmed that miR-577 can regulate TSGA10 and in turn affect cell proliferation in vitro. Additionally, with flow cytometry and manipulation of the mir-577/TSGA10 axis, it was found that mir-577/TSGA10 axis influenced the growth of ESCC through regulating the G1-S phase transition. We also obtained evidence to establish that mir-577/TSGA10 axis activation was always accompanied by inactivation of the p53 pathway or the Rb pathway or both, thus, the latter two pathways are obligatory for progression of ESCCs with mir-577/TSGA10 axis activation. In addition, we found that such an interactive pathway in regulating cancer cell proliferation was restricted to a few cancer types including ESCC, but not uniformly applicable to other cancer types. This newly discovered regulatory mechanism provides a new dimension for ESCC diagnosis and therapy.

Keywords: ESCC, TSGA10, miR-577, G1-S phase transition, p53/p21 pathway, Rb/p16 pathway

Introduction

Esophageal cancer is one of the ten most common cancers worldwide with a gloomy prognosis. The major histological subtype of esophageal cancer in China is esophageal squamous cell carcinoma (ESCC) [1], which has the eighth highest incidence and ranks number six in the cause of cancer death in China [2]. ESCC is well known for its distinct geographic distribution. Linzhou of Henan Province in central China, where this study was conducted, has the highest incidence of ESCC in the world [1]. In spite of years of research, the pathogenesis of ESCC is still poorly understood. Therefore, a better understanding of the molecular mechanism governing its growth and early diagnosis are urgently needed.

TSGA10 was originally classified as a testis-specific protein [3]. Recent studies suggested that it had a broad distribution in normal tissues [4] as well as in a few solid cancers [5-7]. However, the possible roles of TSGA10 in cancer development and growth including ESCC remained unknown. Growing evidence indicated that microRNAs are involved in many cellular events [8, 9] and knowledge of the association between miRNAs and their target genes would enhance our understanding of carcinogenesis [10]. Nevertheless, the possible interaction between TSGA10 and microRNAs has not been elucidated. Deregulation of normal cell cycle

control has been implicated in the development of human cancers. In particular, abnormal expression of genes that control p53 pathway and G1-S phase transition, critical events in cell cycle progression in malignant tumors including ESCC, are frequently observed [11-14].

In this study, we found that miR-577 and TSGA10 formed an interactive regulatory pathway and play a vital role in controlling tumor proliferation and G1-S phase transition in ESCC. We further demonstrated that ESCC with mir-577/TSGA10 axis activation was always accompanied by inactivation of the p53 pathway or the Rb pathway or both.

Materials and methods

Ethics statement

A total of 100 ESCC tumor sample and Normal esophageal tissue samples were obtained from surgical specimens from Anyang Tumor Hospital (Anyang, Henan, China) with approval of the Ethics Committee of Anyang Tumour Hospital. The surgeons obtain the patient's consent and signature to agree to donate their excised tumor tissues for scientific research during preoperative conversations. The whole procedure of consent was approved and documented by the Ethics Committee of Anyang Tumour Hospital. All the samples were conserved in the Molecular Pathology Laboratory of Beijing University Health Science Center. The study protocol was viewed and approved by the Ethics Committee of Beijing University Health Science Center for research use only.

All animal studies were performed in strict accordance with the recommendations in the guidelines for the Animal Care and Use Committee of The Tenth People's Hospital of Shanghai. Permit number: 2011-RES1. The protocol was approved by Science and Technology Commission of Shanghai Municipality (ID: SYXK 2007-0006). The rats were kept at 18°C-26°C on a 12 hours light and dark cycle with free access to water and standard rat chow. They were allowed to acclimatize for a minimum of 1 week. The environment was maintained at a relative humidity of 30%-70%. All surgery was performed under sodium pentobarbital anesthesia, and all efforts were made to minimize suffering

Collection of esophageal tissue specimens and patient information

A total of 100 histopathologically diagnosed Esophageal Squamous Cell Carcinoma obtained from patients treated at Anyang Tumor Hospital (Anyang, Henan, China) from 2008 to 2010 were investigated. Upon surgical resection, esophageal cancers and their corresponding adjacent normal tissues (at least 5 cm from the cancerous tissue) were collected and cut into two parts: one part was processed immediately for RNA exaction or stored in liquid nitrogen for later extraction. The other was fixed in 10% formalin and embedded in paraffin, sectioned at 4 μm in thickness and stained with Hematoxylin and Eosin (H&E).

The 100 cases included 75 men and 25 women, aged 35 to 82 years (median, 58 years), with stage I (7 cases), IIa (23 cases), IIb (25 cases) and III (45 cases) according to UICC. Twenty eight cases ESCC were well differentiated, 42 were moderately differentiated and 30 were poorly differentiated.

Tumor cell lines

To study the function of the mir-577/TSGA10 axis in vitro, a panel of tumor cell lines derived from esophageal, cervix, nasopharynx and bladder cancers were cultured in RPMI 1640 (Invitrogen, Carlsbad, CA) supplemented with 10% FBS (Hy-Clone, Logan, UT) at 37°C in a humidified atmosphere containing 5% CO_2. Detailed information of these tumor cell lines is provided in Supplementary Table 1.

MTS-based assay and Colony Formation Assay

In order to test the growth and viability of tumor cells, the MTS-based assay (Promega, Madison, WI, USA) and Colony Formation Assay were performed [15]. Briefly, about 1,000 or 3,000 (for serum starvation condition) cells were seeded in 96-wellplates and cultured for 24 h. In each group, 5 wells were examined. After addition of 20 μL aliquot of MTS labeling reagent, cells were further incubated for 30 min at 37°C. Cell viability was examined at the indicated time points (0 h, 24 h, 48 h, 72 h, and 96 h). The plates were read at a wavelength of 490 nm. For Colony Formation Assay, 200 cells were seeded per well in 6-well plates and allowed to grow for 14 days. Resulting colonies

were fixed in 70% ethanol and stained with 0.5% crystal violet, the colony numbers were determined using the ImageJ software (National Institutes of Health (NIH), Bethesda, MD, USA).

Mouse models of tumor growth

To investigate tumorigenicity of the ESCC cells with manipulated TSGA10 expression, we employed a nude mouse model. Briefly, a lentivirus-based system was used to specifically down-regulate or up-regulate TSGA10 expression. The recombinant lentiviral plasmids carrying human TSGA10 (pGIPZ-based lentiviral vector) or shRNA-TSGA10 gene (pLK0.1 lentiviral vector) were successfully established and were used to transfect ESCC cell line KYSE150 or EC109. Then, approximately 5×10^6 established cells were orthotopically xenografted in 6–8-week-old male nude mice (Bikai, Shanghai, China). Six mice were included in each group. Tumor volume was monitored weekly for up to 6 weeks and calculated with the formula: $0.5 \times \text{length} \times \text{width}^2$. Six weeks after inoculation, tumor-bearing mice were sacrificed one hour after BrdU injection (50 mg/kg). Tumors were collected, measured, weighted, sectioned, and stained for BrdU [16].

Quantitative real-time PCR (Q-RT-PCR) and western blot analysis (WB)

To examine whether the TSGA10 gene was differentially expressed in ESCC and adjacent non-tumor tissues, we employed Q-PCR. The sequences of the oligonucleotide primers and sequencing are provided in Supplementary Table 2. To test the influence of miR-577/TSGA10 axis on cell cycle regulators, we performed WB. The primary antibodies are described in Supplementary Table 3.

Immunohistochemical staining and analysis

To study the expression and localization of the proteins, IHC was performed on paraffin tissue sections (4 μm) as described previously [17]. Information of the antibodies was provided in Supplementary Table 3. The histologic appearance and staining intensity were examined and scored by two pathologists independently and classified into: absent (scored as -), weak-positive (scored as +), moderately-positive (scored as ++) and strong-positive (scored as +++) staining. We classified 2+ or 3+ expression as positive, and + or - expression as negative.

Cell synchronization and flow cytometry

To investigate whether mir-577/TSGA10 axis influenced the growth of ESCC through regulating cell cycle, cell synchronization and flow cytometry were employed. For cell synchronization, transfected cells were seeded in six-well plates and incubated in serum-deprived media (0.2% FBS) for 72 h. Subsequently, cells were incubated with complete medium (10% FBS) [18]. In order to investigate cell cycle distribution at each time point (0 h, 2 h, 6 h, 10 h, 16 h), flow cytometry was employed and data were analyzed with ModFit software (BD Biosciences, San Jose, CA, USA).

Luciferase reporter assay

To investigate whether miR-577 regulates TSGA10 through the binding site of 3'UTR, we employed a luciferase reporter assay. Different forms of TSGA10 3'UTR (wt-TSGA10 3'UTR; mut-TSGA10 3'UTR) were cloned down-stream to the renilla luciferase gene into the psiCHECK2 vector, and the firefly luciferase gene was used to normalize the reporter activities. Luciferase activities were measured with the Dual-luciferase Reporter Assay System (Promega, Madison, WI, USA).

Transient transfections of microRNAs, anti-miRs, siRNAs or pcDNAs

To manipulate the expressions of miR-577 and TSGA10, Lipofectamine 2000 transfection reagent and Opti-MEM Medium (Invitrogen, Carlsbad, CA, USA) were applied to the transient transfection of microRNA mimics, Anti-miR Inhibitor mimics (Genepharma, Shanghai, China), si-TSGA10 (Sigma-Aldrich, St Louis, MO, USA), and pcDNA3.1 or pcDNA3.1-TSGA10 (2 μg) according to the manufacturer's instructions. The final concentration of microRNA or siRNA used in our study was 50 nM.

To performed a set of experiments in ESCC cell lines to further validate whether miR-577 affects proliferation of ESCC through regulating its potential target TSGA10, a plasmid containing the entire TSGA10 coding sequence

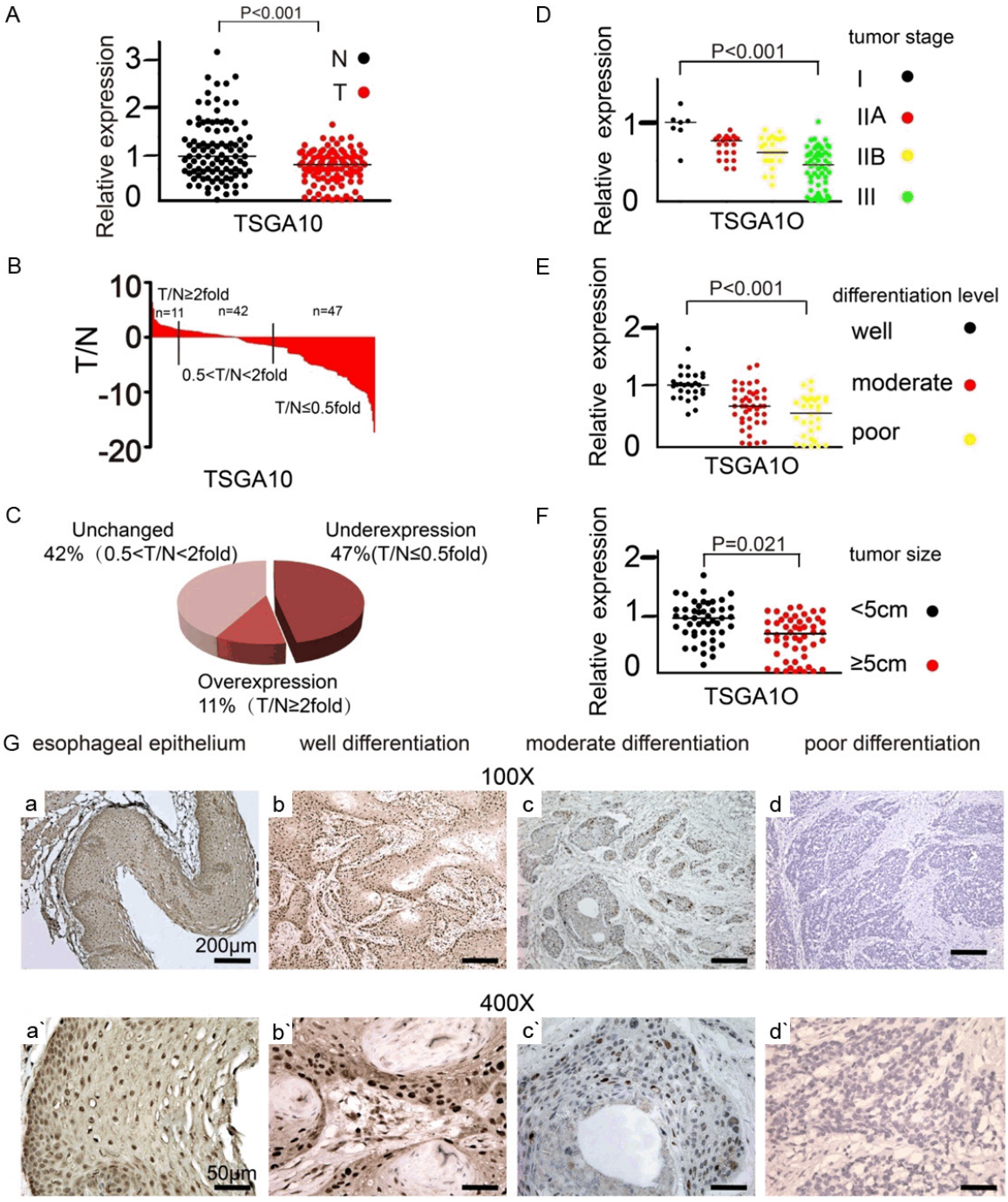

Figure 1. Down-regulation of TSGA10 in ESCC is associated with clinical features. (A) The difference of TSGA10 mRNA expression in tumor samples (T, n = 100) and adjacent esophageal epithelial tissues (N, n = 100) analyzed by Quantitative real-time PCR (Q-PCR). 18 S rRNA served as an internal control. The value of each sample was calculated as -ΔCt: -(Ct TSGA10-Ct 18 S rRNA). The average -ΔCt value of N is set at 1; P < 0.001; Student's t-test. (B) The fold changes of the relative expression of TSGA10 (T/N). Expression of TSGA10 was determined by Q-PCR in 100 paired ESCC tumors (T) and their corresponding esophageal epithelial tissues (N). 18 S rRNA served as an internal control. (T/N) < 0.5 or > 2 was defined as significant. (C) Pie graph shows the percentages of the 100 tumor samples with under-expressed, unchanged, and over-expressed TSGA10. (D-F) Correlation between TSGA10 expression in ESCC tumor samples and different clinical features: stage (D), differentiation state (E), and tumor size (F). TSGA10 expression level was calculated the same as in (A). The average -ΔCt value of "tumors at stage I" (D); "tumors with well differentiation" (E) and "tumors with size < 5 cm in diameter" (F) are set at 1, respectively. (G) Representative IHC photos of TSGA10 expression in normal tissue (a-100× and a`-400×) and ESCC tumors with

different differentiations (b-d-100×; b`-d`-400×). TSGA10 staining was mainly localized within the nucleus of cells in the form of yellow brown granules. All sections were counterstained with hematoxylin.

without the 3'UTR fragment was constructed. This construct can restore TSGA10 and is insensitive to miR-577-mediated repression due to lack of 3'UTR.

BrdU incorporation and immunofluorescence staining

DNA synthesis was assessed with bromodeoxyuridine (BrdU) incorporation which was visualized with immunofluorescence. The primary antibodies were described in Supplementary Table 3. BrdU labeling index was calculated as BrdU-positive cells/total DAPI (4, 6-diamino-2-phenyl indole)-positive cells. Finally, cultures were mounted in ProLong® Gold Anti fade Reagent with DAPI (Invitrogen); and subsequently viewed with a fluorescence microscope or a Zeiss confocal microscope system (Oberkochen, Germany).

Statistical analysis

The relationship between the expression of TSGA10 (mRNA and score of the IHC staining) and clinicopathologic features was tested with χ^2 test. A Student's t-test was performed to compare the differences between treated groups in relation to their paired controls. A *P*-value < 0.05 (denoted by *) was considered statistically significant. (**when P < 0.01). Data analyses were carried out with ImageJ software (National Institutes of Health (NIH), Bethesda, MD, USA), GraphPad Prism 5.0 software (GraphPad software, San Diego, California, USA) and Microsoft Excel (Microsoft, USA).

Results

The expression of TSGA10 gene is related to tumor differentiation, clinical stage and tumor size in ESCC

TSGA10 expression level in tumor samples (T) was found to be significantly lower than that in the adjacent normal tissues (N) (P < 0.001; **Figure 1A**). When matched pairs of ESCC tumors and the adjacent normal tissue were compared, 47% (47 of 100) of the tumors had at least 2-fold reduction in TSGA10 expression (**Figure 1B** and **1C**).

We then investigated the correlation between TSGA10 expression and clinicopathologic features. The results showed that TSGA10 expression level in ESCCs was significantly correlated to clinical stage (P = 0.004), tumor differentiation (P = 0.022), and tumor size (P = 0.003), but not to other clinical features such as age or gender (Supplementary Table 4).

We found that TSGA10 expression in tumors at the advanced stage (stage III) was significantly lower than those at the early stages (stage I, IIA and IIB, **Figure 1D**). Similarly, TSGA10 expression in poorly-differentiated tumors was significantly lower than those of well- or moderately-differentiated tumors (**Figure 1E**); and TSGA10 expression in large tumors (≥ 5 cm in diameter) was significantly lower than those of small tumors (< 5 cm in diameter, **Figure 1F**).

We further examined the expression of TSGA10 in 60 pairs of ESCC tumor/normal tissue sections with IHC. We found that the positive staining of TSGA10 was localized within the nucleus. Moreover, TSGA10 was uniformly expressed in the entire epithelial layer and it was not restricted to the basal cell layer. In addition, the population of the TSGA10 positive cells decreased in number from well differentiated to poorly differentiated cancers (**Figure 1G**). We also observed that under the classification system for staining intensity described in Materials and Methods, when comparing the IHC scores between normal epithelium and the cancer samples, the difference was statistically significant (Supplementary Table 5), the same trend was found for mRNA. Moreover, correlation between TSGA10 and features analyzed with IHC was in line with the mRNA results (Supplementary Tables 6, 7 and 8).

TSGA10 suppresses tumor formation in nude mice

Five ESCC cell lines were tested for correlation between the expression levels of TSGA10 and the rate of cell proliferation. Different cell lines were found to express TSGA10 to different levels with EC-109 and EC-1 cells had the most abundant expressions, followed by EC-9706 and TE-1 cells, and KYSE-150 had the least (Supplementary Figure 1A). With the same

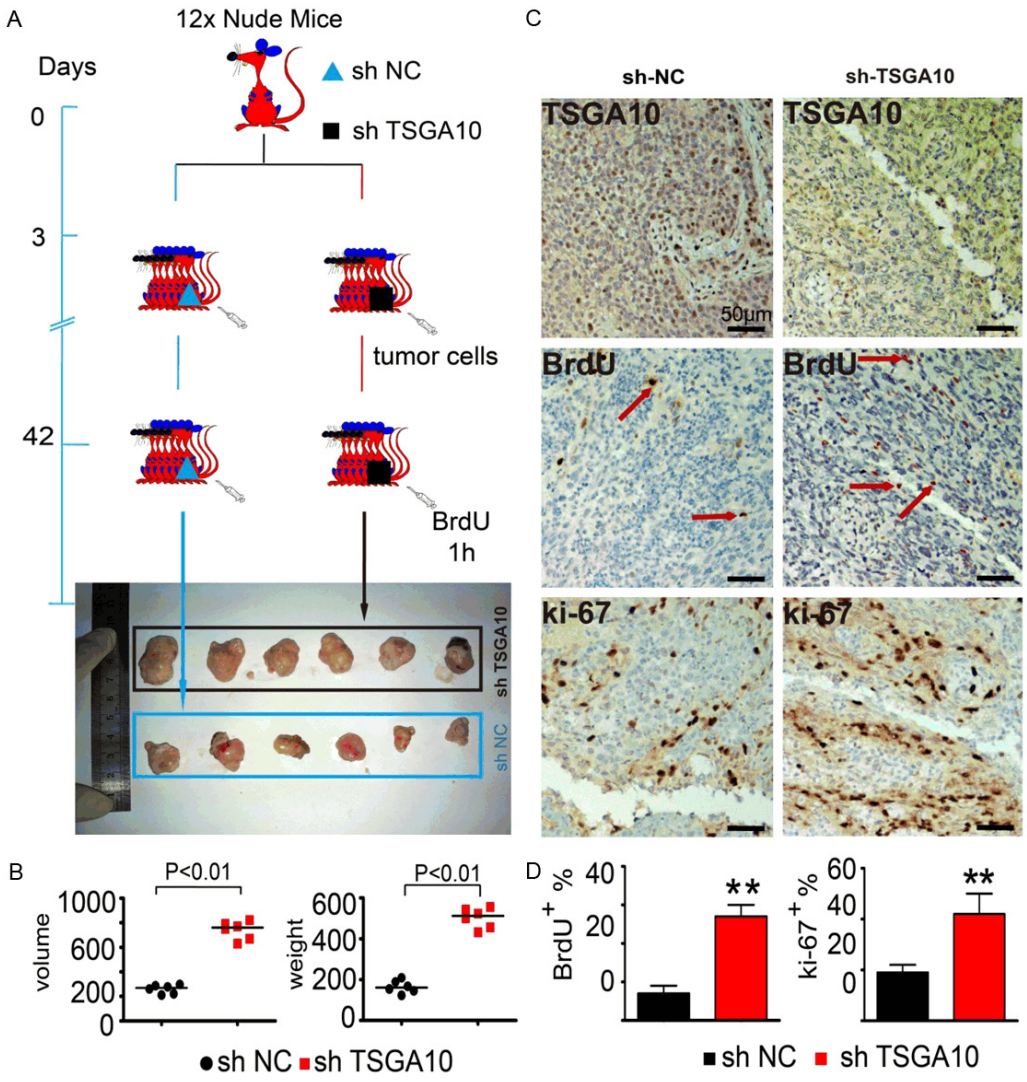

Figure 2. TSGA10 knockdown promoted tumor formation in nude mice xenografts. (A) Schematic presentation of the tumor formation and BrdU injection in nude mice and the representative photos of xenografts. (B) Scatter plots representing s.c. tumor volume and weight. The weight and volume of EC-109 xenografts (TSGA10 knockdown; 511.5 ± 49.1 mg and 760 ± 73.5 mm^3, respectively) are larger than the control (160.5 ± 30.98 mg and 269 ± 36.3 mm^3; $P < 0.01$ for both weight and volume; Student's t-test). (C and D) Typical images (C) and quantification (D) of BrdU or ki-67-positive cells are displayed. The dark brown color indicates BrdU or ki-67-positive nuclei. The scale bar represents 50 μm. Each bar represents the mean ± s.d. of three independent experiments; **, $P < 0.01$.

order but in reverse, KYSE-150 cells had the highest proliferation rate, followed by EC9706 and TE-1, and then EC109 and EC-1 cells had the slowest growth rate (Supplementary Figure 1B).

The effect of TSGA10 in vivo on tumor growth was determined by measuring the volume of tumors each week. Tumor formation was observed subcutaneously in all nude mice at 2 weeks after injection. During a five-week follow-up period, tumor volumes increased. Six weeks following tumor cell implantation and one hour after BrdU injection, we found that tumor volume of the nude mice bearing EC109/sh-TSGA10 cells was significantly larger than that of the controls (**Figure 2A** and **2B**), whereas, the tumor volume of nude mice bearing KYSE150/TSGA10 cells was significantly smaller than that of the controls (Supplementary Figure 1C).

Furthermore, IHC analysis found a marked increase in the staining intensity of ki-67 and

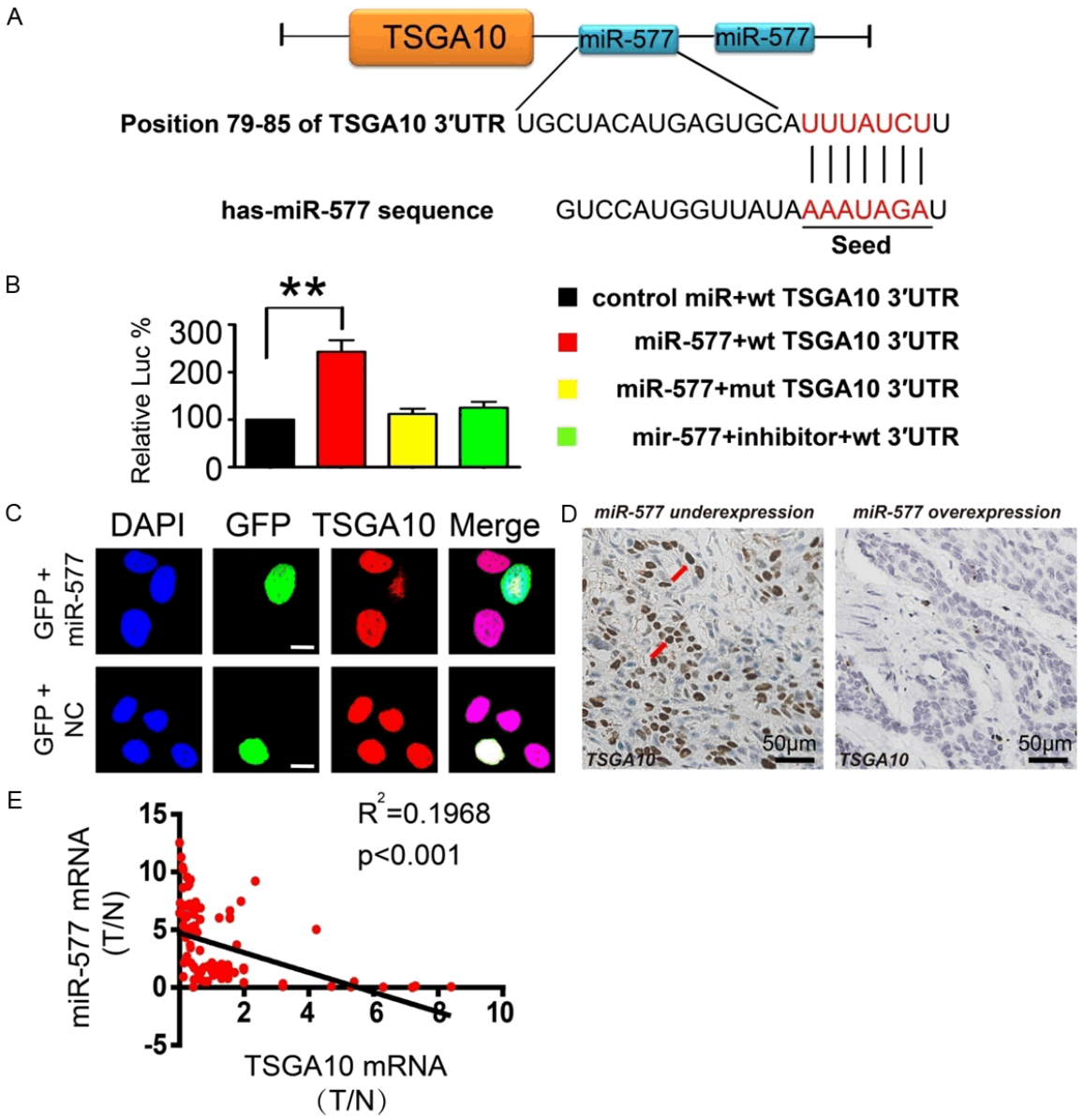

Figure 3. MiR-577 acted as an upstream regulator of TSGA10. A: The public database predicted that TSGA10 might be a target for miR-577, and the 3'UTR of human TSGA10 contains two highly conserved binding sites. B: 293-T cells were transfected with Wt or Mut reporter plasmid and miR-577, negative control, or anti-miR-577 inhibitor. After transfected for 48 h, luciferase activity was measured by a dual-luciferase reporter assay. The result was presented as relative LUC (firefly/renilla luciferase), the relative LUC of control was set at 100%. Each bar represents the mean ± s.d. of three independent experiments; **, $P < 0.01$. C: TSGA10 expression was examined by immunofluorescence analysis. GFP images (green)–miR-577 and GFP images (green)-NC indicate cells with miR-577 over-expression (top) or control (bottom), respectively. Red, TSGA10 protein; blue, DAPI; green, GFP. The scale bar represents 5 μm. D: More TSGA10 staining cells were observed in ESCC tumors with miR-577 under-expression. Red arrows indicated TSGA10-positive cells. E: negative correlation between the expression of miR-577 and TSGA10 in 100 tumor samples ($R^2 = 0.1968$; $p < 0.001$). The relative expression of miR-577 and TSGA10 were quantified using Q-PCR and normalized by U6 or 18 S.

BrdU-positive cells in xenografts with TSGA10 down-regulation as compared to controls (**Figure 2C** and **2D**), whereas xenografts with TSGA10 up-regulation gave the opposite effect (Supplementary Figure 1D and 1E).

MiRNA-577 fine tunes TSGA10 to form a pathway in ESCC progression

With the open-access software of targetscan [19], we found two highly conserved binding

Table 1. IHC scores of TSGA10 in miR-577 low or miR-577 high group

	TSGA10 Negative	TSGA10 Positive	Total
miR-577 low	8	18	26
miR-577 high	50	24	74
Total	58	42	100

Negative correlation between the expression of miR-577 and TSGA10 in 100 ESCC tumors. The relative expression of miR-577 was quantified using Q-PCR and normalized by U6. TSGA10 was evaluated by IHC staining. P = 0.001.

sites for miR-577 (**Figure 3A**), which had not been reported previously. In order to validate our prediction, a luciferase reporter assay was further performed. As shown in **Figure 3B**, miR-577 co-transfection dramatically increased the relative luciferase activity of the vector encoding the wt-TSGA10 3'UTR, but not the vector with mut-TSGA10 3'UTR. Moreover, the relative luciferase activity remained as low as in the control group in the presence of anti-miR-577 inhibitor (**Figure 3B**). These data showed that miR-577 was TSGA10's upstream regulator and targeted TSGA10 at its 3'UTR. In addition, we found that the expression level of TSGA10 decreased as the expression of miR-577 increased in the cell lines EC-109, EC-1, EC-9706 and KYSE-150 (Supplementary Figure 2A). Moreover, when EC-109 cells were treated with miR-577 mimics the expression of TSGA10 decreased. Conversely, when KYSE-105 cells were treated with miR-577 inhibitor, the expression of TSGA10 increased (Supplementary Figure 2B), thus confirming a negative correlation between the expression of endogenous miR-577 and TSGA10. We further confirmed their correlation at the protein level with immunofluorescence staining (**Figure 3C**).

We also found a negative correlation between the two in ESCCs. Based on the expression level of miR-577 in the 100 ESCC tumor samples, we classified the ESCC into two groups, i.e. miR-577 low (26 samples) and miR-577 high (74 samples). Much more TSGA10-positive cells were in miR-577 low group than in miR-577 high group (**Figure 3D**). Moreover, much higher proportion of miR-577 low cases was TSGA10 positive than that of miR-577 high cases (**Table 1**). The expression of TSGA10 and miR-577 in the 100 tumor samples analyzed with Pearson Correlation also showed a negative correlation between the two (**Figure 3E**).

Mir-577/TSGA10 interaction regulates ESCC cell proliferation in vitro

MiR-577 over-expression in EC-109 resulted in a significant increase in cell proliferation when compared to the control (**Figure 4A**). This pattern was similar to that when TSGA10 was knocked down in EC-109 (Supplementary Figure 3A and 3B). Moreover, over-expression of miR-577 in EC-109 accelerated colony formation (**Figure 4B**). Once again, this was the same to the results when TSGA10 was knocked down in EC-109 (Supplementary Figure 3C). Finally, the proliferation increase or colony formation in response to miR-577 over-expression was both reversed by TSGA10 restoration (**Figure 4A** and **4B**).

In consistent to this trend, inhibition of miR-577 and over-expression of TSGA10 in KYSE-150 cells had a similar impact on cell proliferation (Supplementary Figure 3D-F) and colony formation (Supplemental Figure 3G and 3H). On the other hand, attenuation of TSGA10 expression significantly reversed the reduced growth rate and the reduction in the number of colonies upon miR-577 inhibition in KYSE150 cells (Supplementary Figure 3D and 3G).

Mir-577/TSGA10 pathway influences G1-S phase transition in ESCC cells in vitro

We firstly synchronized mir-577 manipulated ESCC cells at the G0/G1 stage by serum starvation, and re-started cell cycle with serum stimulation, then collected cells at specified time intervals, and analyzed the cell cycle distributions (**Figure 5A**) [20-23].

In cell cycle analysis, cells with mir-577 over-expression had a lower proportion at the G0/G1 phase and a higher proportion at the S phase at 2 h - 6 h after serum addition when compared to the control. This indicates that cells with mir-577 over-expression underwent a more rapid G1-S phase transition. Moreover, mir-577 over-expressing cells finished the first cell cycle at 6 h and began to enter into the next cycle. However, control cells did not complete the first cycle until 10 h or later (**Figure 5B**). In contrast, cells with mir-577 inhibition had a higher proportion at the G0/G1 phase and a

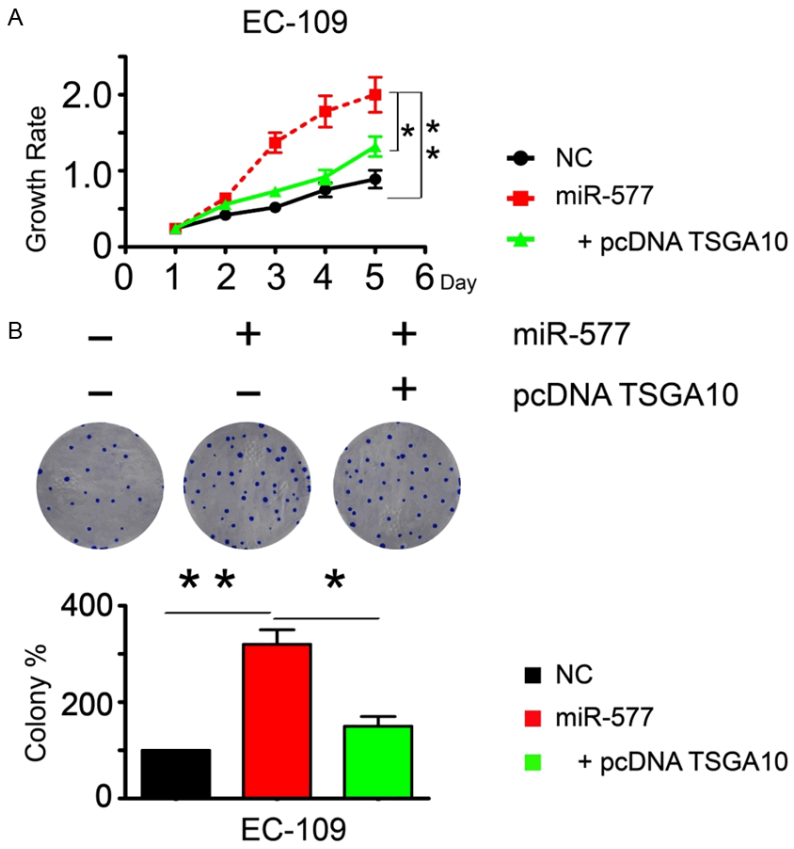

Figure 4. The activation of miR-577/TSGA10 pathway promoted EC-109 cell proliferation *in vitro*. A: EC109 cells were transfected with NC, miR-577 mimics, or miR-577 mimics along with the expression plasmid pcDNA-TSGA10 (contains TSGA10 open reading frame without 3'UTR), respectively. The proliferative capability of each group was determined by MTS-based assay at every 24 h after seeding for 5 days. The proliferation curve was generated based on the absorbance (OD490). B: For the colony formation, representative dishes of crystal violet-stained colonies were photographed (upper). Colony quantification (bottom) is presented as colony number in percentage of the treatment group relative to control group (set at 100%). Each bar represents the mean ± s.d. of three independent experiments; *, P < 0.05; **, P < 0.01.

lower proportion at the S phase at 2 h - 6 h after serum addition when compared to the control. As a result, cells were accumulated at the G0/G1 phase and failed to enter the S phase (Supplementary Figure 4A).

The proportion of cells entering S phase were also examined by monitoring bromodeoxyuridine (BrdUrd) incorporation in synchronized cells following serum stimulation. Consistent with our previous observations, much more mir-577 over-expressing cells had incorporated BrdU than controls following 6 hours of serum stimulation (**Figure 5C**), whereas mir-577 inhibition significantly delayed the entry into S phase with less cells incorporating BrdU over the same time period than controls (Supplementary Figure 4B).

Additionally, TSGA10 restoration rescued the G1/S transition caused by miR-577 over-expression (Supplementary Figure 4C). On the other hand, attenuation of TSGA10 expression significantly reversed the G1/S arrest caused by miR-577 inhibition (Supplementary Figure 4D).

Inactivation of Rb and p53 pathways in ESCCs with mir-577/TSGA10 pathway activation

We found marked decreases in the expression of molecules in p53 pathway including p53 and p21Waf1/Cip1 as well as key components of G1/S transition control pathway including Rb and p16 in EC-109 cells in response to mir-577 over-expression (**Figure 6A**). In contrary, we found an opposite pattern of gene expression in response to mir-577 inhibition in KYSE-150 cells (**Figure 6B**). Furthermore, the restoration or attenuation of TSGA10 could reverse the genes alterations caused by mir-577 over-expression or down-regulation (**Figure 6A** and **6B**).

We then examined abnormalities of genes involved in these regulatory pathways according to their protein accumulation detected by IHC in a series of ESCC samples. The tumors were divided into two groups: mir-577/TSGA10 axis activation group featured by mir-577 over-expression and TSGA10 down-regulation, and the inactivation group.

Among the 27 ESCCs with mir-577/TSGA10 axis activation, 20 tumors had Tp53 protein nuclear accumulation (p = 0.014) and 25 had

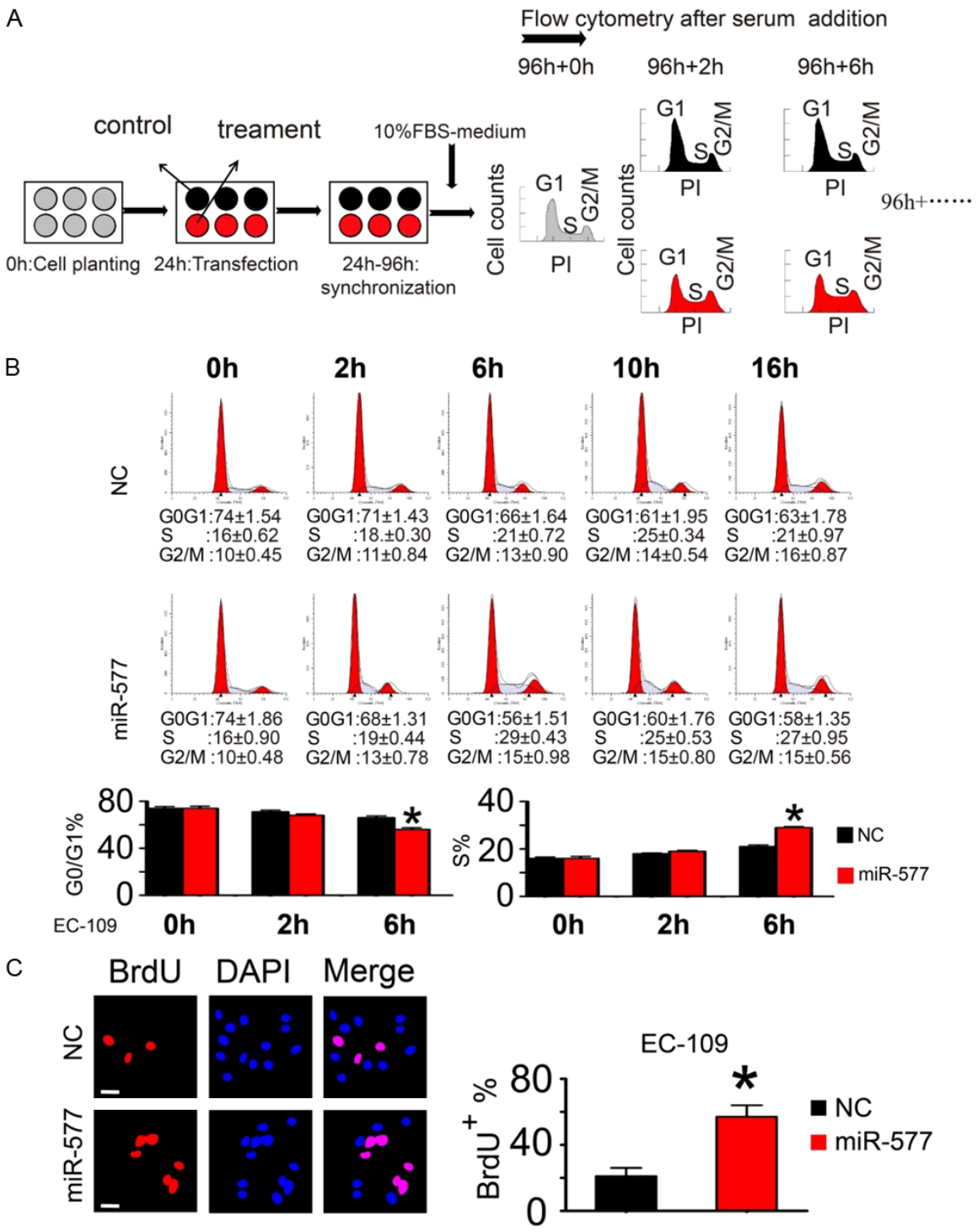

Figure 5. The activation of miR-577/TSGA10 pathway promoted G1-S phase transition in EC-109 cells *in vitro*. A: Schematic diagram of cell synchronization and cell cycle distribution analysis. ESCC cells were firstly transfected with microRNA mimics or plasmids, next synchronized in serum-deprived medium for 72 h, then incubated in 10% FBS medium at the 96th hour. After that, cell were stained by PI and collected by flow cytometry at the specified time intervals. B: Representing flow cytometry diagrams showing cell cycle distribution of control EC109 cells or cells with mir-577 over-expression treatment at indicated time points (0 h, 2 h, 6 h, 10 h, 16 h) after serum addition (upper panel). Bar plots showing the percentage of cells in G0/G1 and S phase (lower panel). C: BrdU uptake showing the DNA synthesis the 6 h after serum addition. Typical images (upper) and quantification (lower) of BrdU-positive cells are displayed. There was a significantly different percentage of BrdU-positive cells in the treatment group when

compared to the control group. The scale bar represents 100 μm. Each bar represents the mean ± s.d. of three independent experiments; *, P < 0.05.

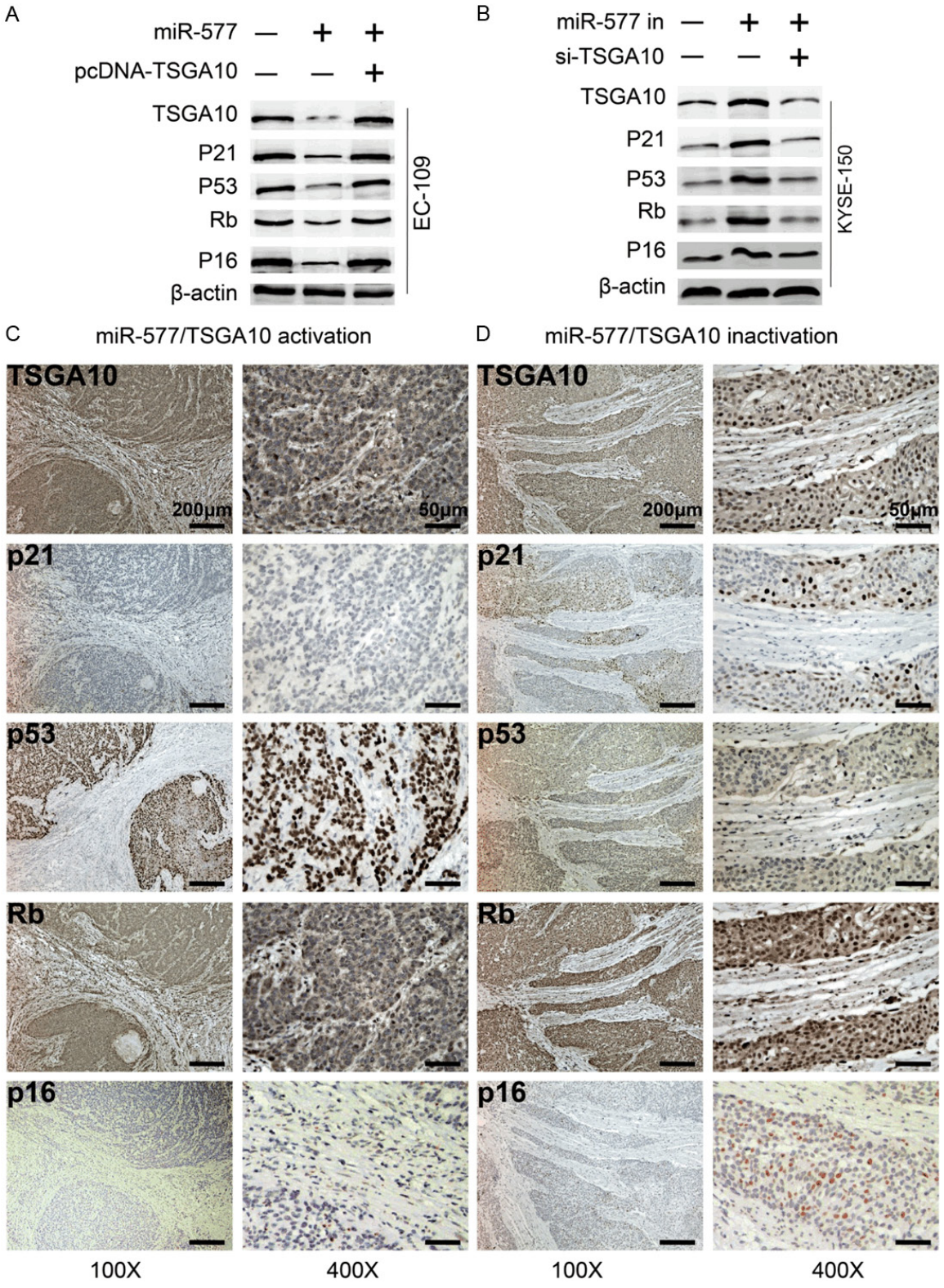

Figure 6. Effect of mir-577/TSGA10 axis on Tp53/p21Waf1/Cip1 and Rb/p16INK4a signaling pathways. (A) EC109 cells were transfected with NC, miR-577 mimics, or miR-577 mimics along with the expression plasmid pcDNA-TS-

GA10 (contains TSGA10 open reading frame without 3'UTR), respectively. Immunoblotting for TSGA10, p21, p53, Rb and p16 using lysates from each group with anti-β-actin antibody to normalize for differences in protein loading. (B) KYSE150 cells were transfected with NC, miR-577 inhibitor, or inhibitor along with si-TSGA10, respectively. Immunoblotting for TSGA10, p21, p53, Rb and p16 using lysates from each group with anti-β-actin antibody to normalize for differences in protein loading. (C and D) Representative photomicrographs showing the immunohistochemical staining patterns of proteins in Rb and p53 Pathways in ESCC samples with mir-577/TSGA10 pathway activation (C) and mir-577/TSGA10 pathway inactivation (D). We performed TSGA10, p53, p21, Rb and p16 immunohistochemical staining using serial sections from the same paraffin-embedded tissue blocks. Tissue section with mir-577/TSGA10 activation (C) showed intense nuclear staining for p53 and negative staining for TSGA10, p21, Rb and p16, respectively. Tissue section with mir-577/TSGA10 inactivation (D) showed opposite staining patterns.

negative nuclear staining of p21/Cip1 ($p < 0.001$). Moreover, 20 tumors had deregulated p53 pathway with both events ($p < 0.001$) and 25 tumors had either TP53 accumulation or negative nuclear p21/Cip1 staining ($p = 0.002$, Supplementary Table 9). Among the same group, 21 tumors had negative nuclear Rb staining ($p = 0.011$) and 18 had negative nuclear p16 staining ($p = 0.035$). Moreover, 17 tumors had deregulated G1-S transition control pathway with both events ($p = 0.006$) and 22 had either negative nuclear staining of Rb or p16 ($p = 0.048$, Supplementary Table 9). When all data combined and compared, 16 ESCCs with mir-577/TSGA10 pathway activation had dual inactivation of RB and p53 pathways by simultaneously negative staining of p21, p16, Rb and accumulation of p53 ($p < 0.001$, Supplementary Table 9).

In summary, we identified a statistically significant association between the activation alteration of the mir-577/TSGA10 pathway and inactivation of p53 pathway either by TP53 accumulation or negative nuclear p21/Cip1 staining ($p = 0.002$) or both ($p < 0.001$). We also identified a significant correlation between the activation of the mir-577/TSGA10 pathway and deregulated G1-S transition control pathway either by negative nuclear staining of Rb or p16 ($p = 0.048$) or both ($p = 0.006$). The association between mir-577/TSGA10 pathway activation and dual inactivation of Rb and p53 pathways was also significant by simultaneously negative nuclear staining of p21, p16, Rb and p53 protein accumulation ($p < 0.001$, Supplementary Table 10).

Representative photomicrographs of IHC staining indicated a consistent pattern of significantly negative immunoreactivity of p21, p16 and Rb and P53 protein accumulation in tumors with mir-577/TSGA10 activation (**Figure 6C**). In contrast, there is an opposite pattern of immunoreactivity in tumors with mir-577/TSGA10 inactivation (**Figure 6D**).

MiR-577 functions as a promoter of rapid proliferation in multiple cancer cells and promotes cell cycle progression under nutrition-deprived condition

In investigating the interaction of miR-577 and TSGA10 and their biological effects, miR-577 was also found to promote cell proliferation when examining other cell lines derived from cervical cancer (Hela and ca ski), nasopharynx cancer (5-8f) and bladder cancer (EJ, T24, J82), (Supplementary Figure 5A and 5B). Furthermore, in EJ and 5-8f cell lines (bladder and nasopharynx), the miR-577/TSGA10 regulatory axis behaved the same way as ESCC (**Figure 7A**). However, in ca ski cell line (cervical), they behaved differently (Supplementary Figure 5C), i.e. attenuation of TSGA10 expression could not reverse the reduced growth rate caused by miR-577 inhibition.

On the other hand, we found that miR-577 protected tumor cells against the negative effect induced by serum deprivation and maintained cell cycle progression. We used EC109 as a model. After incubation with serum-deprived medium (0.2% FBS) for 80 h, or complete serum starvation condition (0% FBS) for 100 h, the cells became floated with considerable cell loss. In contrast, cell with miR-577 over-expression continued to adhere to each other without obvious cell floating up to 100 h (**Figure 7B**). Additionally, consistent with this morphological observation, cells with miR-577 over-expression had much higher viability than the control cells as time prolonged following serum deprivation (Supplementary Figure 5D). Moreover, miR-577 over-expression appeared to preserve DNA synthesis of cells under serum-deprived condition than the control cells (**Figure 7C**). Furthermore, miR-577 might be beneficial for tumor cells to escape

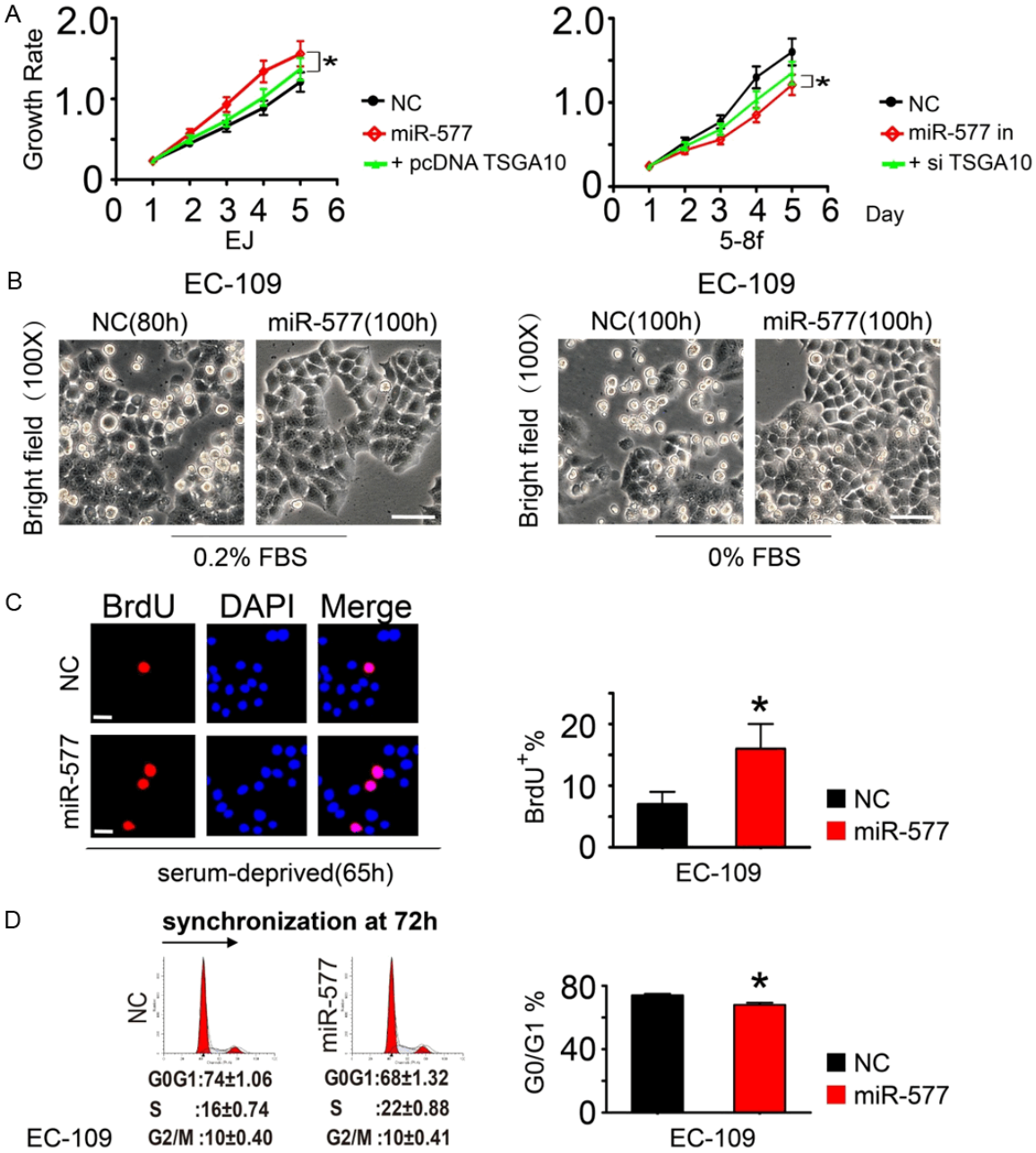

Figure 7. The miR-577/TSGA10 regulatory axis behaved the same way as ESCC in EJ and 5-8f cancer cells and mir-577promoted cell cycle progression under nutrition-deprived condition. (A) (Left) EJ cells were transfected with NC, miR-577 mimics, or miR-577 mimics along with the expression plasmid pcDNA-TSGA10 (contains TSGA10 open reading frame without 3'UTR), respectively. The proliferative capability of each group was determined by MTS-based assay at every 24 h after seeding for 5 days. The proliferation curve was generated based on the absorbance (OD490). (Right) 5-8f cells were transfected with NC, miR-577 inhibitor, or inhibitor along with si-TSGA10, respectively. The proliferative capability of each group was determined by MTS-based assay at every 24 h after seeding for 5 days. (B) Control EC109 cells or cells with miR-577 over-expression exhibit different morphologies under serum-deprived or serum-null conditions at indicated time points. The scale bar represents 100 μm. (C) BrdU incorporation showing the DNA synthesis state of EC109 cells after the 65 h serum starvation. Typical images (left) and quantification (right) of BrdU-positive cells are displayed. Cell counting showed a significantly different percentage of BrdU-positive cells with miR-577 over-expression compared to the control. The scale bar represents 100 μm. (D) miR-577 promotes G1-S phase transition of EC109 cells under serum starvation (Left). Bar plots show the significant less percentage of cells in G0/G1 phase in EC109 cells with miR-577 over-expression under serum starvation (Right). Each bar represents the mean ± s.d. of three independent experiments; *, $P < 0.05$.

the G0/G1 boundary and re-enter the cell cycle under starvation (**Figure 7D**). However, this protective effect appeared not to involved TSGA10 gene (data not shown).

Discussion

This study provided the first evidence that a molecular regulatory mechanism involving the expression of a potential tumor suppressor gene TSGA10 and an oncomir miR-577 as its direct upstream regulator might play a role in ESCC biology.

Interaction of miR-577 and TSGA10 regulated ESCC proliferation

The function of TSGA10 has not been well established although it has been suggested to act as an oncogene [6, 7, 24, 25]. In this study, however, we obtained evidence to suggest that it acted as a tumor suppressor gene in ESCC and its down-regulation was significantly associated with increased malignancy of this cancer. Moreover, increased expression of TSGA10 inhibited, while its knockdown promoted, tumor formation in vivo in nude mice. These were consistent with the previous studies reporting an increased expression of TSGA10 during spermatogenesis and involvement in active cell division, differentiation and proliferation [4, 24].

As the expression level of TSGA10 was suggested to be post-transcriptionally regulated [3, 7, 25], we searched for factors that can regulate its expression. A microRNA miR-577 was found to be a likely candidate as there were two binding sites in the TSGA10 gene for miR-577. Moreover, an increase of miR-577 led to a decrease in TSGA10 and an increase in cell proliferation. When the decreased TSGA10 was compensated by an over-expression of TSGA10, the cell proliferation slowed. In reverse, when miR-577 was down-regulated, TSGA10 was increased and cell proliferation was decreased. Similarly but in reverse, when the increase of TSGA10 was inhibited the cell proliferation increased. Additionally, expression levels of miR-577 and TSGA10 were found to be negatively correlated to each other in ESCC. These evidences suggested that miR-577 and TSGA10 formed an interactive regulatory pathway and play a pivotal role in controlling tumor proliferation in ESCC.

Mir-577/TSGA10 axis influenced the growth of ESCC through regulating G1-S phase transition

It has been reported that well-orchestrated cell cycle is necessary for normal growth, whereas disorganized cell cycle distribution contributes to rapid proliferation [22, 23]. This raised the question that whether mir-577/TSGA10 axis influenced the growth of ESCC through regulating cell cycle progression.

In this study, we obtained evidence to establish that cells with mir-577 over-expression and then TSGA10 down-regulation underwent a more rapid G1-S phase transition than control cells, as evidenced by persistently decreased numbers of cells in G0/G1 stage and the increased numbers in S phase during specified time intervals after serum stimulation.

In contrast, cells with mir-577 inhibition and then TSGA10 up-regulation exhibited a phenomenon of G0/G1 accumulation in comparison to the controls as evidenced by the persistently maintained higher proportion of cell numbers in G0/G1 phase and the lower proportion in S phase during specified time intervals after serum stimulation.

These notions were derived with flow cytometry of the two ESCC cell lines that had been manipulated with either activation or inactivation of mir-577/TSGA10 axis, thus providing further evidence for this regulating mechanism.

Dual inactivation of Rb and p53 pathways cooperated with activation of mir-577/TSGA10 pathway to promote tumor progression of ESCC

To elucidate possible regulatory mechanisms of the cell cycle progression by mir-577/TSGA10 pathway, the expression of multiple well-characterized cell cycle related genes were examined [26-29]. We found marked alterations in the endogenous expression of p53 pathway members as well as key components of G1/S transition control system in ESCC cells in response to changes of mir-577/TSGA10 pathway, thus providing a possible connection between mir-577/TSGA10 pathway and the two pathways, which are critical events in the progression of malignant tumors including ESCC. We further investigated their associations

in the progression of ESCC and demonstrated that ESCC with mir-577/TSGA10 axis activation was always accompanied by inactivation of the p53 pathway or the Rb pathway or both, illustrating the cooperative effects of these two systems on the roles of mir-577/TSGA10 pathway in cell cycle progression of ESCC.

It is intriguing that another series of tumors showed mir-577/TSGA10 axis activation without any components alteration in either p53/p21 pathway or Rb pathway, and this was interpreted as due to the alteration of other components of these pathways.

In this study, a tumor was identified as p53 or Rb pathway inactivation by alteration of even one component of this regulatory pathway, which supports the idea that individual genetic abnormality should be viewed as ways of disrupting the whole cell signaling but not as simply abrogating functions of a single gene [29, 30], also supports the idea that abnormalities of each component may have approximately equivalent effects [11, 29].

Given the significant association between mir-577/TSGA10 pathway activation and TP53 nuclear accumulation alone, in this study, we also identified a significant association between the mir-577/TSGA10 pathway activation and TP53 mutation, since a good correlation is known to exist between p53 protein accumulation and the presence of TP53 gene mutations in ESCC [14, 31, 32]. This novel finding is exciting, since the activation of mir-577/TSGA10 pathway may give insight into p53 mutation, one of the most frequent genetic lesions associated with ESCC progression [31].

Limitations of mir-577/TSGA10 axis in cell types as well as in biological behaviors of cancers

In investigating the interaction of miR-577 and TSGA10 and their biological effects, miR-577 was also found to induce as well as required for other tumor cells in culture to proliferate, thus, miR-577 might be a general promoter for rapid tumor progression. However, the above interaction between miR-577 and TSGA10 may be tissue and cancer type specific. MiR-577 was found to induce at least four cancer types to proliferate, but it appeared that only in some cancer cell types TSGA10 played a role. In other cells TSGA10 appeared not involved, indicating that TSGA10 might not be the only target mediating the proliferative effects of miR-577, and the effect exerted by miR-577 might not always go through TSGA10 in all cancer types.

Another interesting observation in our study was that miR-577 had a protective effect on tumor cells during nutrition starvation. At initial stages of tumor development, tumor cells often have to face harsh physiological microenvironments, such as lack of nutrition or ischemia [33]. However, miR-577 might be beneficial for tumor cells to escape the G0/G1 boundary and re-enter the cell cycle under conditions of nutrition deprivation. This persistent cell cycle progression would facilitate uncontrolled cell growth in carcinogenesis and renders ESCC cells more aggressive [34]. However, the protective role of miR-577 appeared not to involve TSGA10 gene expression but may through other mechanisms [35-43]. Therefore, the axis formed by miR-577 and TSGA10 found in ESCC might not be universal and has limitations not only in cell types but also in biological behaviors of cancer.

Acknowledgements

We thank Professor Cizhong Jiang (The University of Tongji, Shanghai, China) for critical reading of the manuscript and for helpful comments and suggestions. We are grateful to Professor Kuisheng Chen (Department of Pathology, The University of Zhengzhou, Henan, China) for providing ESCC cell lines. All authors critically discussed the results and the manuscript. We thank our colleagues for excellent technical assistance and helpful suggestions. This work was supported by grants from the National Natural Science Foundation of China (No. 81030033, 30971150 to J.G.)

Disclosure of conflict of interest

The authors declare no conflict of interest.

Address correspondence to: Dr. Jiang Gu, Molecular Pathology Laboratory and Guangdong Provincial Key Laboratory of Infectious Diseases and Molecular Immunopathology, Shantou University Medical College, Shantou 515041, China. Tel: 86-13502752606; Fax: 86-754-8895 0293; E-mail: gujiangmd@126.com; jguemailbox@gmail.com; Dr.

Fenyong Sun, Department of Clinical Laboratory Medicine, Shanghai Tenth People's Hospital of Tongji University, Shanghai 200072, China. Tel: 86-21-66300588; Fax: 86-21-66300588; E-mail: fenyongsunijcep@126.com; Dr. Xiang Yuan, Department of Pathology, School of Basic Medical Science, Peking University, Beijing 100083, China. E-mail: yuanxiang1105@126.com

References

[1] Ma S, Bao JY, Kwan PS, Chan YP, Tong CM, Fu L, Zhang N, Tong AH, Qin YR, Tsao SW, Chan KW, Lok S and Guan XY. Identification of PTK6, via RNA sequencing analysis, as a suppressor of esophageal squamous cell carcinoma. Gastroenterology 2012; 143: 675-686, e671-612.

[2] Chen ZL, Zhao XH, Wang JW, Li BZ, Wang Z, Sun J, Tan FW, Ding DP, Xu XH, Zhou F, Tan XG, Hang J, Shi SS, Feng XL and He J. microRNA-92a promotes lymph node metastasis of human esophageal squamous cell carcinoma via E-cadherin. J Biol Chem 2011; 286: 10725-10734.

[3] Modarressi MH, Behnam B, Cheng M, Taylor KE, Wolfe J and van der Hoorn FA. Tsga10 encodes a 65-kilodalton protein that is processed to the 27-kilodalton fibrous sheath protein. Biol Reprod 2004; 70: 608-615.

[4] Behnam B, Modarressi MH, Conti V, Taylor KE, Puliti A and Wolfe J. Expression of Tsga10 sperm tail protein in embryogenesis and neural development: from cilium to cell division. Biochem Biophys Res Commun 2006; 344: 1102-1110.

[5] Theinert SM, Pronest MM, Peris K, Sterry W and Walden P. Identification of the testis-specific protein 10 (TSGA10) as serologically defined tumour-associated antigen in primary cutaneous T-cell lymphoma. Br J Dermatol 2005; 153: 639-641.

[6] Dianatpour M, Mehdipour P, Nayernia K, Mobasheri MB, Ghafouri-Fard S, Savad S and Modarressi MH. Expression of Testis Specific Genes TSGA10, TEX101 and ODF3 in Breast Cancer. Iran Red Crescent Med J 2012; 14: 722-726.

[7] Behnam B, Chahlavi A, Pattisapu J and Wolfe J. TSGA10 is Specifically Expressed in Astrocyte and Over-expressed in Brain Tumors. Avicenna J Med Biotechnol 2009; 1: 161-166.

[8] Kong YW, Ferland-McCollough D, Jackson TJ and Bushell M. microRNAs in cancer management. Lancet Oncol 2012; 13: e249-258.

[9] Wang Y, Baskerville S, Shenoy A, Babiarz JE, Baehner L and Blelloch R. Embryonic stem cell-specific microRNAs regulate the G1-S transition and promote rapid proliferation. Nat Genet 2008; 40: 1478-1483.

[10] Farazi TA, Hoell JI, Morozov P and Tuschl T. MicroRNAs in Human Cancer. Adv Exp Med Biol 2013; 774: 1-20.

[11] Bardeesy N, Bastian BC, Hezel A, Pinkel D, DePinho RA and Chin L. Dual inactivation of RB and p53 pathways in RAS-induced melanomas. Mol Cell Biol 2001; 21: 2144-2153.

[12] Sheahan S, Bellamy CO, Dunbar DR, Harrison DJ and Prost S. Deficiency of G1 regulators P53, P21Cip1 and/or pRb decreases hepatocyte sensitivity to TGFbeta cell cycle arrest. BMC Cancer 2007; 7: 215.

[13] Abel EV and Aplin AE. FOXD3 is a mutant B-RAF-regulated inhibitor of G(1)-S progression in melanoma cells. Cancer Res 2010; 70: 2891-2900.

[14] Hui CM, Cheung PY, Ling MT, Tsao SW, Wang X, Wong YC and Cheung AL. Id-1 promotes proliferation of p53-deficient esophageal cancer cells. Int J Cancer 2006; 119: 508-514.

[15] Hosono Y, Yamaguchi T, Mizutani E, Yanagisawa K, Arima C, Tomida S, Shimada Y, Hiraoka M, Kato S, Yokoi K, Suzuki M and Takahashi T. MYBPH, a transcriptional target of TTF-1, inhibits ROCK1, and reduces cell motility and metastasis. EMBO J 2012; 31: 481-493.

[16] Bussink J, Kaanders JH, Rijken PF, Martindale CA and van der Kogel AJ. Multiparameter analysis of vasculature, perfusion and proliferation in human tumour xenografts. Br J Cancer 1998; 77: 57-64.

[17] Ansari D, Rosendahl A, Elebro J and Andersson R. Systematic review of immunohistochemical biomarkers to identify prognostic subgroups of patients with pancreatic cancer. Br J Surg 2011; 98: 1041-1055.

[18] Cifuentes E, Croxen R, Menon M, Barrack ER and Reddy GP. Synchronized prostate cancer cells for studying androgen regulated events in cell cycle progression from G1 into S phase. J Cell Physiol 2003; 195: 337-345.

[19] Gebeshuber CA, Zatloukal K and Martinez J. miR-29a suppresses tristetraprolin, which is a regulator of epithelial polarity and metastasis. EMBO Rep 2009; 10: 400-405.

[20] Huang Q, Li J, Wang F, Oliver MT, Tipton T, Gao Y and Jiang SW. Syncytin-1 modulates placental trophoblast cell proliferation by promoting G1/S transition. Cell Signal 2013; 25: 1027-1035.

[21] Duronio RJ and Xiong Y. Signaling Pathways that Control Cell Proliferation. Cold Spring Harb Perspect Biol 2013; 5: a008904.

[22] Song L, Wang L, Li Y, Xiong H, Wu J, Li J and Li M. Sam68 up-regulation correlates with, and its down-regulation inhibits, proliferation and

tumourigenicity of breast cancer cells. J Pathol 2010; 222: 227-237.
[23] Xia J, Wu Z, Yu C, He W, Zheng H, He Y, Jian W, Chen L, Zhang L and Li W. miR-124 inhibits cell proliferation in gastric cancer through down-regulation of SPHK1. J Pathol 2012; 227: 470-480.
[24] Mobasheri MB, Modarressi MH, Shabani M, Asgarian H, Sharifian RA, Vossough P and Shokri F. Expression of the testis-specific gene, TSGA10, in Iranian patients with acute lymphoblastic leukemia (ALL). Leuk Res 2006; 30: 883-889.
[25] Roghanian A, Jones DC, Pattisapu JV, Wolfe J, Young NT and Behnam B. Filament-associated TSGA10 protein is expressed in professional antigen presenting cells and interacts with vimentin. Cell Immunol 2010; 265: 120-126.
[26] Blagosklonny MV, Prabhu NS and El-Deiry WS. Defects in p21WAF1/CIP1, Rb, and c-myc signaling in phorbol ester-resistant cancer cells. Cancer Res 1997; 57: 320-325.
[27] Guo W, Zou YB, Jiang YG, Wang RW, Zhao YP and Ma Z. Zinc induces cell cycle arrest and apoptosis by upregulation of WIG-1 in esophageal squamous cancer cell line EC109. Tumour Biol 2011; 32: 801-808.
[28] Madan E, Gogna R, Kuppusamy P, Bhatt M, Pati U and Mahdi AA. TIGAR induces p53-mediated cell-cycle arrest by regulation of RB-E2F1 complex. Br J Cancer 2012; 107: 516-526.
[29] Ichimura K, Bolin MB, Goike HM, Schmidt EE, Moshref A and Collins VP. Deregulation of the p14ARF/MDM2/p53 pathway is a prerequisite for human astrocytic gliomas with G1-S transition control gene abnormalities. Cancer Res 2000; 60: 417-424.
[30] den Hollander P and Kumar R. Dynein light chain 1 contributes to cell cycle progression by increasing cyclin-dependent kinase 2 activity in estrogen-stimulated cells. Cancer Res 2006; 66: 5941-5949.
[31] Wagata T, Shibagaki I, Imamura M, Shimada Y, Toguchida J, Yandell DW, Ikenaga M, Tobe T and Ishizaki K. Loss of 17p, mutation of the p53 gene, and overexpression of p53 protein in esophageal squamous cell carcinomas. Cancer Res 1993; 53: 846-850.
[32] Chen C, Chang YC, Liu CL, Chang KJ and Guo IC. Leptin-induced growth of human ZR-75-1 breast cancer cells is associated with up-regulation of cyclin D1 and c-Myc and down-regulation of tumor suppressor p53 and p21WAF1/CIP1. Breast Cancer Res Treat 2006; 98: 121-132.
[33] Thomas R and Kim MH. HIF-1α: A key survival factor for serum-deprived prostate cancer cells. Prostate 2008; 68: 1405-1415.
[34] Hanahan D and Weinberg RA. Hallmarks of cancer: the next generation. Cell 2011; 144: 646-674.
[35] Thomas R and Kim MH. HIF-1 alpha: a key survival factor for serum-deprived prostate cancer cells. Prostate 2008; 68: 1405-1415.
[36] Yin W, Cheepala S, Roberts JN, Syson-Chan K, DiGiovanni J and Clifford JL. Active Stat3 is required for survival of human squamous cell carcinoma cells in serum-free conditions. Mol Cancer 2006; 5: 15.
[37] Budanov AV, Shoshani T, Faerman A, Zelin E, Kamer I, Kalinski H, Gorodin S, Fishman A, Chajut A, Einat P, Skaliter R, Gudkov AV, Chumakov PM and Feinstein E. Identification of a novel stress-responsive gene Hi95 involved in regulation of cell viability. Oncogene 2002; 21: 6017-6031.
[38] Chen ZX and Pervaiz S. Involvement of cytochrome c oxidase subunits Va and Vb in the regulation of cancer cell metabolism by Bcl-2. Cell Death Differ 2010; 17: 408-420.
[39] Yan J, Tian J, Zheng Y, Han Y and Lu S. Selenium promotes proliferation of chondrogenic cell ATDC5 by increment of intracellular ATP content under serum deprivation. Cell Biochem Funct 2012; 30: 657-663.
[40] Pang T, Wakabayashi S and Shigekawa M. Expression of calcineurin B homologous protein 2 protects serum deprivation-induced cell death by serum-independent activation of Na+/H+ exchanger. J Biol Chem 2002; 277: 43771-43777.
[41] Liew JC, Tan WS, Alitheen NB, Chan ES and Tey BT. Over-expression of the X-linked inhibitor of apoptosis protein (XIAP) delays serum deprivation-induced apoptosis in CHO-K1 cells. J Biosci Bioeng 2010; 110: 338-344.
[42] Hsu YY, Liu CM, Tsai HH, Jong YJ, Chen IJ and Lo YC. KMUP-1 attenuates serum deprivation-induced neurotoxicity in SH-SY5Y cells: roles of PKG, PI3K/Akt and Bcl-2/Bax pathways. Toxicology 2010; 268: 46-54.
[43] Castorina A, Giunta S and D'Agata V. Protective effect of the dopamine D(3) receptor agonist (7-OH-PIPAT) against apoptosis in malignant peripheral nerve sheath tumor (MPNST) cells. Int J Oncol 2010; 37: 927-934.

Supplementary Table 1

Cell lines

EC109 EC9706 EC1	ESCC	Provided by Professor Kuisheng Chen (Department of Pathology,The University of Zhengzhou,Henan, China)
TE-1 KYSE150	ESCC	the Cell Bank of the Chinese Academy of Sciences (Shanghai, China)
EJ T24 J82	Transitional carcinoma of bladder	
Hela ca ski	Squamous cell carcinoma of the cervix	BioHermes (Jiangsu,China)
5-8F	Nasopharyngeal squamous cell carcinoma	

Supplementary Table 2

Primers

Name	5'-3'
TSGA10-F	agacaactaggaacagagcg
TSGA10-R	gatcgatggtgagcacgttc
mir577RT	ctcaactggtgtcgtggagtcggcaattcagttgagcaggtac
mir577F	acactccagctgggtagataaaatattggtac
mir577R	ctcaactggtgtcgtgga
U6 F	ctcgcttcggcagcaca
U6 R	aacgcttcacgaatttgcgt
18S rRNA F	cctggataccgcagctagga
18S rRNA R	gcggcgcaatacgaatgcccc

Supplementary Table 3

Primary Antibody		
Polyclonal mouse Anti-TSGA10	Abcam	IHC/ICC/WB
Monoclonal mouse Anti-p16INK4a		IHC/WB
Monoclonal rabbit Anti-TSGA10	Sigma-Aldrich	IHC/ICC/WB
Monoclonal mouse Anti-BrdU		BrdU incorporation
Monoclonal rabbit Anti-Tp53 (7F5)	Cell Signaling Technology	IHC/WB
Monoclonal rabbit Anti-p21 Waf1/Cip1 (12D1)		IHC/WB
Monoclonal mouse Anti-Rb (4H1)		IHC/WB
Monoclonal mouse Anti-β-actin	Santa Cruz	WB
Secondary Antibody		
Anti-mouse IgG (H+L), F(ab')2 Fragment (Alexa Fluor® 488 Conjugate)	Cell Signaling Technology	ICC
FITC-conjugated goat anti mouse secondary antibodies	Sigma-Aldrich	BrdU incorporation
Goat anti-Rabbit IRDye 800CW （ODYSSEY）	LI-COR	WB
Goat anti-Mouse IRDye 800CW（ODYSSEY）		WB
Polyclonal Goat Anti-Mouse Immunoglobulins	Dako	IHC
DAPI (4',6-Diamidino-2-Phenylindole, Dilactate)	Invitrogen	ICC BrdU incorporation

Supplementary Table 4

Correlation of TSGA10 mRNA level with clinicopathologic features

Characteristic	Total (n = 100)	TSGA10 Expression		P
		low	high	
Age				
<60	42	28	14	0.416
≥60	58	43	15	
Gender				
Female	25	18	7	0.899
Male	75	53	22	
Differentiation				
well	28	17	11	0.022
Moderate	42	27	15	
Poor	30	27	3	
Gross Pathology				
Fungating	33	22	11	0.571
Medullary	53	40	13	
Others	14	9	5	
Position				
Upper	12	8	4	0.842
Middle	63	46	17	
Lower	25	17	8	
T Classification				
T1 T2	9	5	4	0.542
T3	71	52	19	
T4	20	14	6	
N Classification				
N0	54	36	18	0.301
N1	46	35	11	
TNM Stage				
I	7	2	5	0.004
II A	23	14	9	
II B	25	16	9	
III	45	39	6	
Tumor size(cm)				
<5	53	31	22	0.003
≥5	47	40	7	

The 100 ESCC patients were classified as TSGA10-high group and TSGA10-low group by the 75th percentiles of $2^{-\triangle\triangle Ct}$. Pathological grades and tumor sizes are determined by the pathologists. Tumor stages are classified according to the TNM classification of the American Joint Committee on Cancer and the International Union. The association between TSGA10 expression and the clinical features were analyzed. $\chi 2$ test was used, $P<0.05$ was statistically significant.

Supplementary Tables 5-8

The difference of TSGA10 protein expression in paired tumors and adjacent esophageal epithelial tissues analyzed by IHC staining

TSGA10	negative		positive	
	–	+	++	+++
Normal	7		53	
ESCC	39		21	

χ2 test P<0.001

IHC analysis of the correlation between TSGA10 staining intensity and the clinical features (tumor differentiation, tumor stage, and tumor size)

TSGA10	(-)	(+)	(+ +)	(+ + +)
Tumor size(cm)				
<5	4(16%)	4(16%)	5(20%)	12(48%)
≥5	9(36%)	7(28%)	8(32%)	3(12%)

χ2 test P=0.033

TSGA10	(-)	(+)	(+ +)	(+ + +)
TNM Stage				
I	0(0%)	1(14.3%)	2(28.6%)	4(57.1%)
IIA	8(53.3%)	3(20%)	3(20%)	1(6.6%)
IIB	8(53.3%)	4(26.7%)	2(13.3%)	1(6.6%)
III	11(73.4%)	3(20%)	1(6.6%)	0(0%)

P=0.009

TSGA10	(-)	(+)	(+ +)	(+ + +)
Differentiation				
well	1(5%)	3(15%)	7(35%)	9(45%)
Moderate	8(40%)	4(20%)	5(25%)	3(15%)
Poor	12(60%)	3(15%)	4(20%)	1(5%)

P=0.006

Supplementary Table 9

The profile of p53 pathway and G1-S transition control pathway gene abnormalities in ESCCs with mir-577/TSGA10 pathway activation and inactivation

		p53 pathway genes				G1-S transition control genes			
		P21/Cip 1		TP53		Rb		p16	
miR-577-TSGA10		Negative[c]	Positive[d]	Negative	Positive	Negative	Positive	Negative	Positive
1	(O)[a]	−			+++	−		−	
2	(O)	−			+++	−		−	
3	(O)	−			+++	−		−	
4	(O)	−			+++	−		−	
5	(O)	−			+++	−		−	
6	(O)	−			+++	−		−	
7	(O)	−			+++	−		−	
8	(O)	−			+++	−		+	
9	(O)	−			+++	−			++
10	(O)	−			+++	−			++
11	(O)	−			++	−		−	
12	(O)	−			++	−		−	
13	(O)	−			++	−		−	
14	(O)	−			++	+		+	
15	(O)	−			++	+		+	
16	(O)	−			++		+++	+	
17	(O)	+			+++	+		+	
18	(O)	+			+++		++		++
19	(O)	+			++	−		−	
20	(O)	+			++	+		−	
21	(O)	+		+		−			+++
22	(O)	+		+		+			+++
23	(O)	+		−			+++		++
24	(O)	+		−			++		++
25	(O)	+		−			++		++
26	(O)		++	−			++		++
27	(O)		+++	−		+		+	
28	(X)[b]		+++	−			+++		+++
29	(X)		+++	−			+++		+++
30	(X)		+++	−			+++		+++
31	(X)		+++	−			+++		+++
32	(X)		+++	−			++		+++
33	(X)		+++	−		+			+++
34	(X)		+++	+			+++		++
35	(X)		+++	+			+++		++
36	(X)		+++	+		−		−	
37	(X)		+++		+++		++		++
38	(X)		+++		+++	+		−	
39	(X)		+++		++	−			+++
40	(X)		++	−			+++		++
41	(X)		++	−			+++	−	
42	(X)		++	+			++		+++
43	(X)		++		+++	+		+	
44	(X)		++		+++	+			++
45	(X)	+		−			+++		+++
46	(X)	+		−			+++		+++
47	(X)	+		+			++		++
48	(X)	+		+		−		−	
49	(X)	+			+++		++		++
50	(X)	+			+++	−		−	
51	(X)	+			++	−		+	
52	(X)	−		−		−			+++
53	(X)	−		+		+		−	
54	(X)	−		+		+		−	
55	(X)	−			+++		++	+	
56	(X)	−			+++	−			++
57	(X)	−			++	−			++
58	(X)	−			++		++	+	
59	(X)	−			++		++	−	
60	(X)	−			++	−		−	

a:(O),miR-577 is overexpression(by q-PCR,T/N>2 fold) and TSGA10 is negative(by IHC, -/+)

b:(X),miR-577 is downexpression or unchange (by q-PCR,T/N<2 fold) or TSGA10 is positive (by IHC,++/+++)

c:Negative(-/+)

d:Positive(++/+++)

Supplementary Table 10

The significant association between mir-577/TSGA10 pathway activation and dual inactivation of p53 and Rb pathways

		P53 pathway genes				G1-S transition control genes			
		P21/Cip 1		TP53		Rb		p16	
	Total (n=60)	Negative[c]	Positive[d]	Negative	Positive	Negative	Positive	Negative	Positive
miR-577-TSGA10 (O)[a]	27	25(92.6%)	2(17.4%)	7(25.9%)	20(74.1%)	21(77.8%)	6(22.2%)	18(66.7%)	9(33.3%)
miR-577-TSGA10 (X)[b]	33	16(48.5%)	17(51.5%)	19(57.6%)	14(42.4%)	15(45.5%)	18(54.5%)	13(39.4%)	20(60.6%)

a:(O),miR-577 is overexpression(by q-PCR,T/N>2 folds) and TSGA10 is negative(by IHC, -/+)

b:(X),miR-577 is downexpression or unchange (by q-PCR,T/N<2 folds) or TSGA10 is positive (by IHC,++/+++)

c:Negative(-/+)

d:Positve(++/+++)

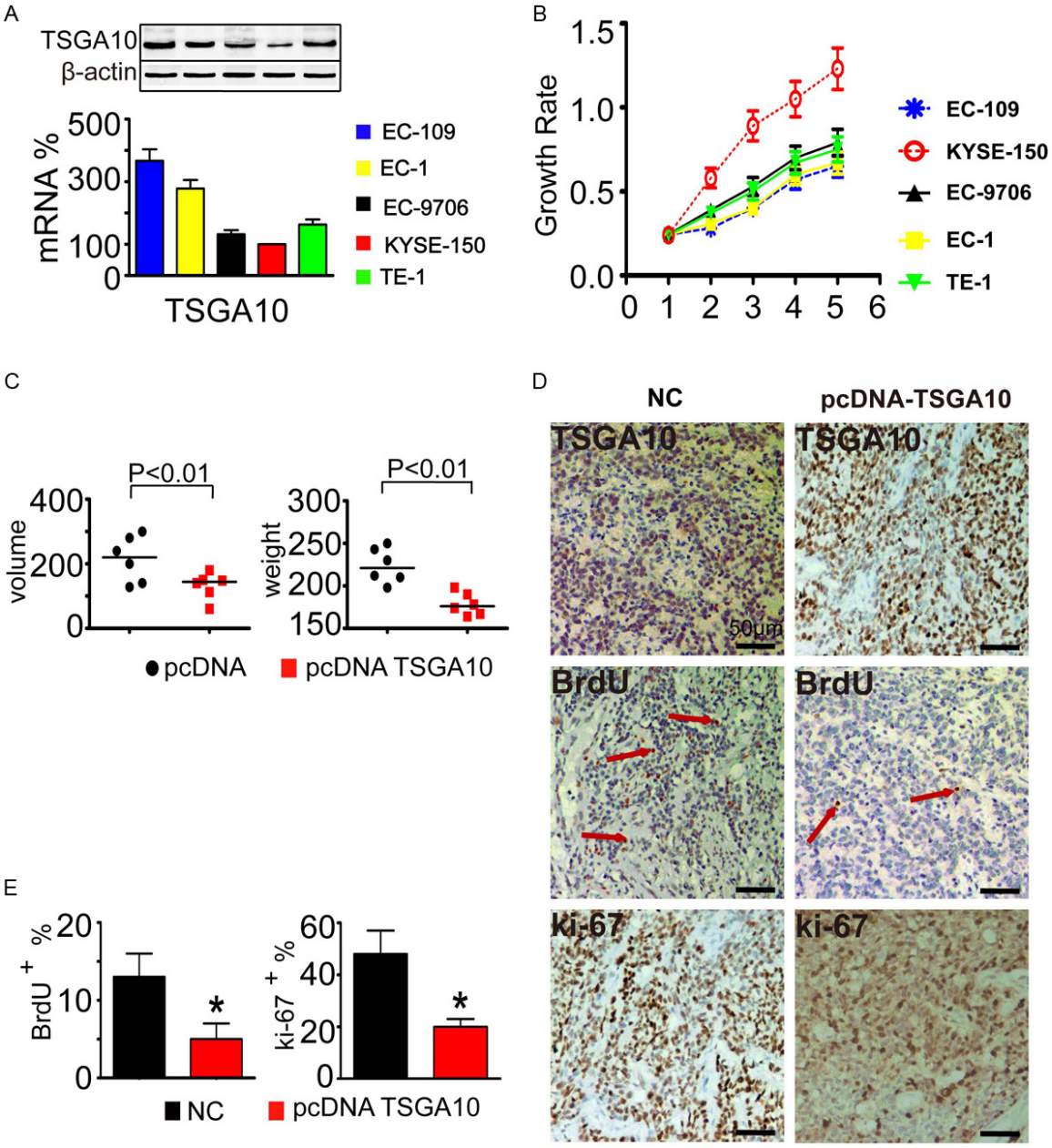

Supplementary Figure 1. TSGA10 over-expression suppressed tumor formation in nude mice xenografts. (A) Endogenous expression level of TSGA10 in ESCC cell lines analyzed by western blot and Q-PCR. β-actin and 18 S rRNA and served as internal controls. The mRNA results were presented as relative TSGA10 expression, the relative value of KYSE-150 was set at 100%. (B) The proliferative capability of each ESCC cell line was determined by MTS-based assay at every 24 h after seeding for 5 days. The proliferation curve was generated based on the absorbance (OD490). (C) Scatter plots representing s.c. tumor volume and weight. The weight and volume of KYSE-150 xenografts (TSGA10 over-expression; 176 ± 13.23 mg and 274 ± 22.9 mm^3, respectively) are smaller than the control (221 ± 20.43 mg and 310 ± 35.7 mm^3; $P < 0.01$; Student's t-test). (D and E) Typical images (D) and quantification (E) of BrdU or ki-67-positive cells are displayed. The dark brown color indicates BrdU or ki-67-positive nuclei. The scale bar represents 50 μm. Each bar represents the mean ± s.d. of three independent experiments; *, $P < 0.05$.

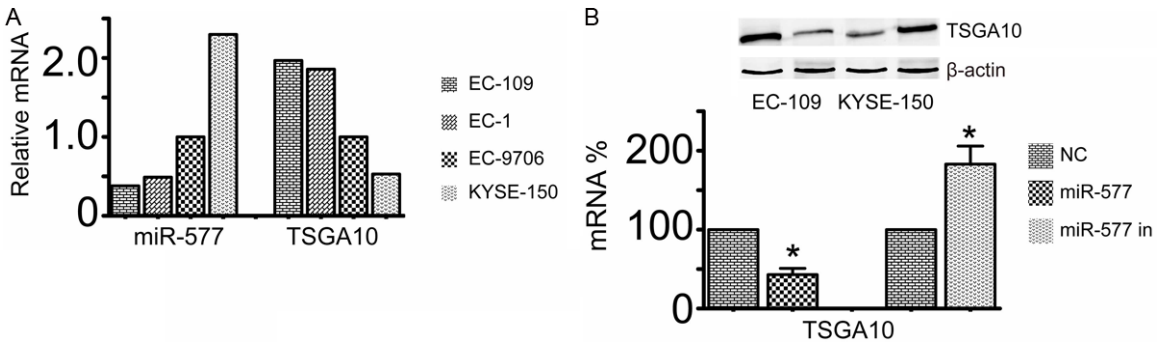

Supplementary Figure 2. The expression of miR-577 and TSGA10 in ESCC cell lines is negatively correlated to each other. A: The endogenous expressions of miR-577 and TSGA10 in ESCC cell lines were quantified by Q-PCR, with RNU6B or 18 S rRNA served as internal control. The relative expressions in EC9706 are both set at 1. B: ESCC cells were transfected with miR-577 mimics or anti-miR-577 inhibitor (50 nmol) for 72 h. TSGA10 expressions were measured by western blotting and Q-PCR. The relative TSGA10 mRNA expressions of NC were set at 100%. Each bar represents the mean ± s.d. of three independent experiments; *, $P < 0.05$.

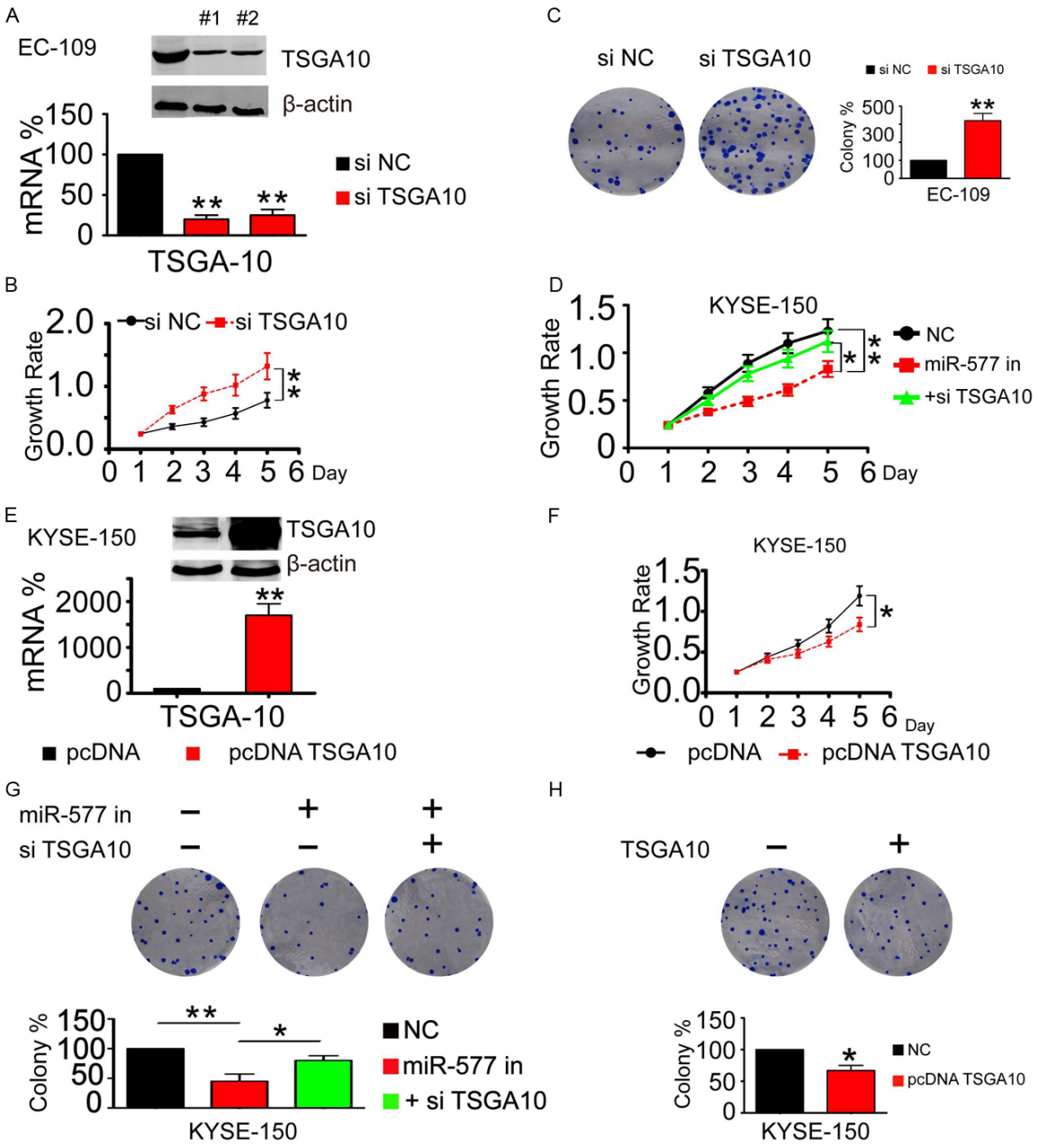

Supplementary Figure 3. The inactivation of miR-577/TSGA10 pathway suppressed KYSE-150 cell proliferation *in vitro*. (A) Q-PCR and Western blot showing the expression of TSGA10 in EC109 cell line after its silencing. The mRNA results were presented as relative TSGA10 expressions, the relative values of control was set at 100%. si NC: si negative control. (B and C) The effect of TSGA10 silencing on EC109 cell proliferation was determined by MTS-based assay (B) and colony formation assay (C). (D and G) KYSE-150 cells were transfected with NC, miR-577 inhibitor, or inhibitor along with si-TSGA10, respectively. The proliferative capability of each group was determined by MTS-based assay at every 24 h after seeding for 5 days (D) and and colony formation assay (G). (E) Q-PCR and Western blot showing the expression of TSGA10 in KYSE150 cell line after its over-expression. The mRNA results were presented as relative TSGA10 expressions, the relative values of control was set at 100%. (F and H) The effect of TSGA10 over-expression on KYSE150 cell proliferation was determined by MTS-based assay (F) and colony formation assay (H). Each bar represents the mean ± s.d. of three independent experiments; *, $P < 0.05$; **, $P < 0.01$.

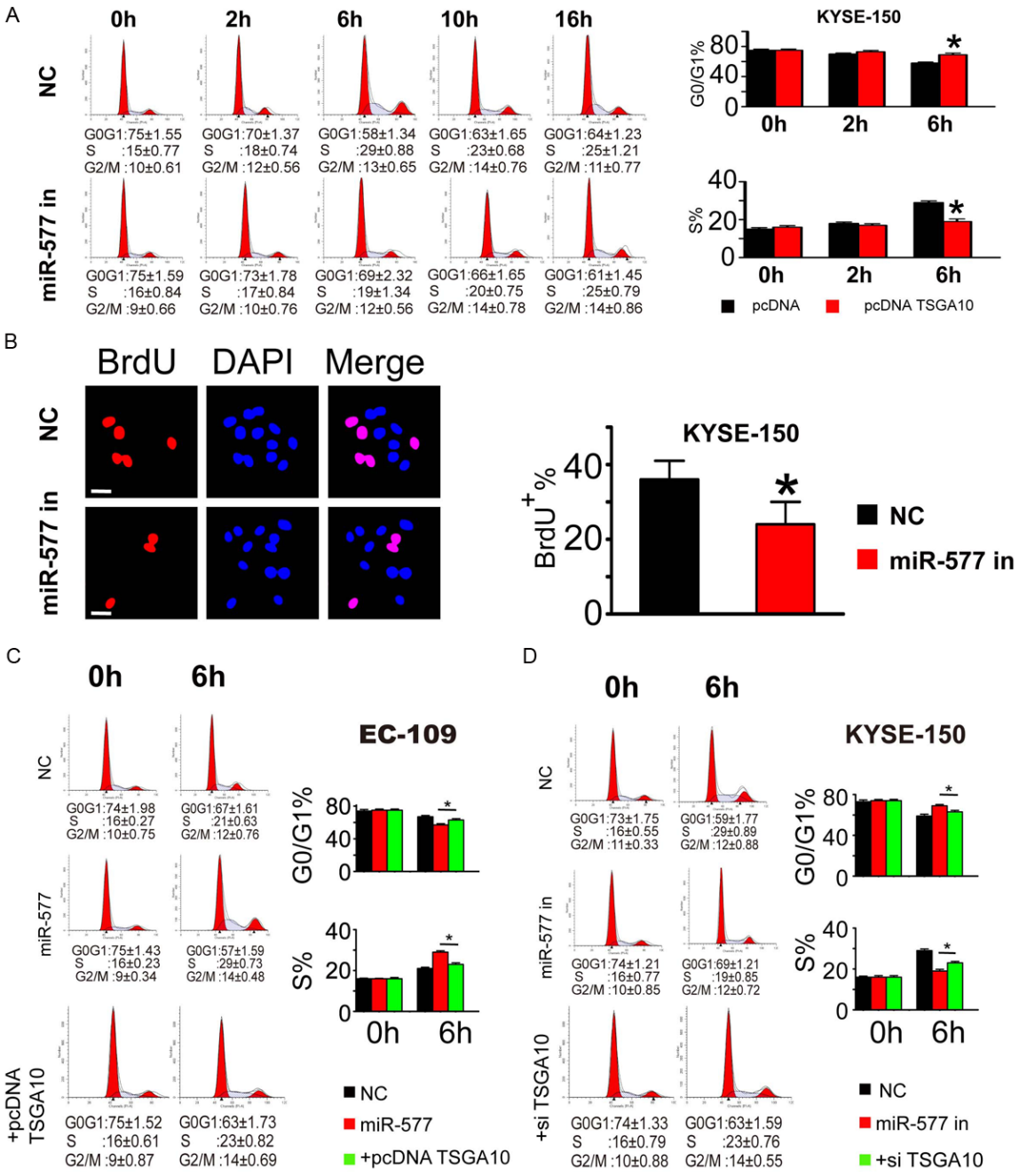

Supplementary Figure 4. The inactivation of miR-577/TSGA10 pathway caused G0/G1 checkpoint accumulation in KYSE-150 cells *in vitro*. A: Representing flow cytometry diagrams showing cell cycle distribution of control KYSE150 cells or cells with mir-577 inhibition at indicated time points (0 h, 2 h, 6 h, 10 h, 16 h) after serum addition (left panel). Bar plots showing the percentage of cells in G0/G1 and S phase (right panel). B: BrdU uptaken showing the DNA synthesis after the 6 h serum addition. Typical images (left) and quantification (right) of BrdU-positive cells are displayed. Cell counting showed a significantly different percentage of BrdU-positive cells in the treatment group compared to the control group. The scale bar represents 100 μm. C: Representing flow cytometry diagrams showing cell cycle distribution of control EC109 cells or cells transfected with miR-577 mimics or miR-577 mimics along with pcDNA-TSGA10 (lack of 3'UTR) at indicated time points (0 h, 6 h) after serum addition (left panel). Bar plots showing the percentage of cells in G0/G1 and S phase (right panel). D: Representing flow cytometry diagrams showing cell cycle distribution of control KYSE150 cells or cells transfected with miR-577 inhibitor or inhibitor along with si-TSGA10 at indicated time points (0 h, 6 h) after serum addition (left panel). Bar plots showing the percentage of cells in G0/G1 and S phase (right panel). Each bar represents the mean ± s.d. of three independent experiments; *, $P < 0.05$.

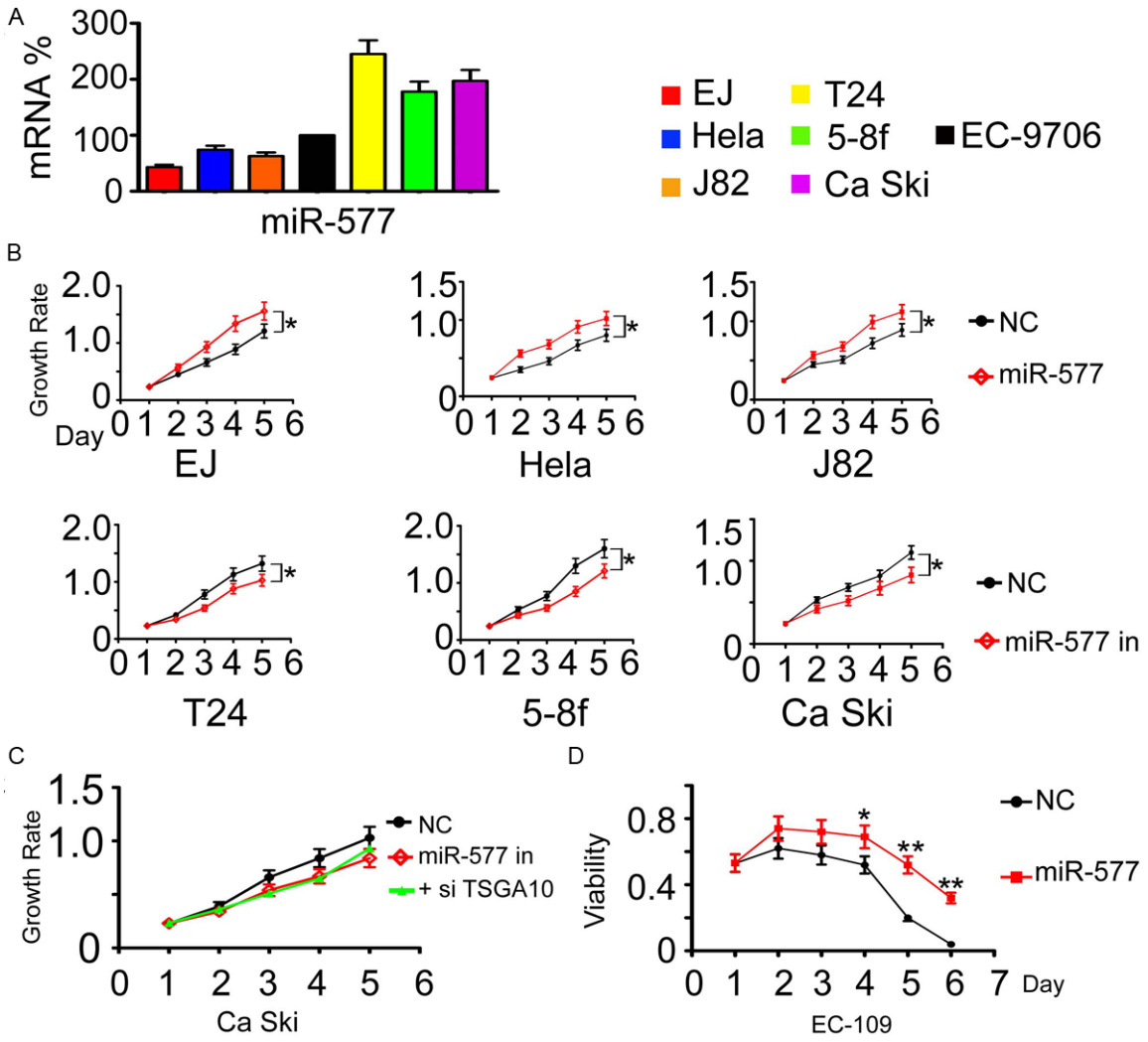

Supplementary Figure 5. MiR-577 functioned as a general promoter of rapid proliferation in multiple cancer cells and maintained cell viability under nutrition-deprived environment. A: Endogenous expression of miR-577 in multiple cancer cell lines analyzed by Q-PCR. RNU6B served as internal controls. The mRNA results were presented as relative miR-577 expression. The relative value of EC9706 was set at 100%. B: MTS-based assay showing the effect of miR-577 manipulation on the proliferative capability of a panel of tumor cells from cervix (Hela, Ca Ski), nasopharynx (5-8f) and bladder cancers (EJ, J82, T24), the proliferation curve was generated based on the absorbance and times. C: Ca Ski cells were transfected with NC, miR-577 inhibitor, or inhibitor along with si-TSGA10, respectively. The proliferative capability of each group was determined by MTS-based assay at every 24 h after seeding for 5 days. D: Time course of miR-577-maintained cell viability under serum-deprived condition. 3,000 cells transfected with miR-577 or NC were seeded in 96-well plates and cultured for 24 h. Cell viability was detected at the indicated time points using the MTS assay. Each bar represents the mean ± s.d. of three independent experiments; *, $P < 0.05$; **, $P < 0.01$.